



Balance Functions of Identified Hadrons in Au+Au Collisions at 200 GeV

Nandita Raha
Postdoc Fellow, Wayne State University
12/12/2022

Seminar – University of Illinois, Chicago

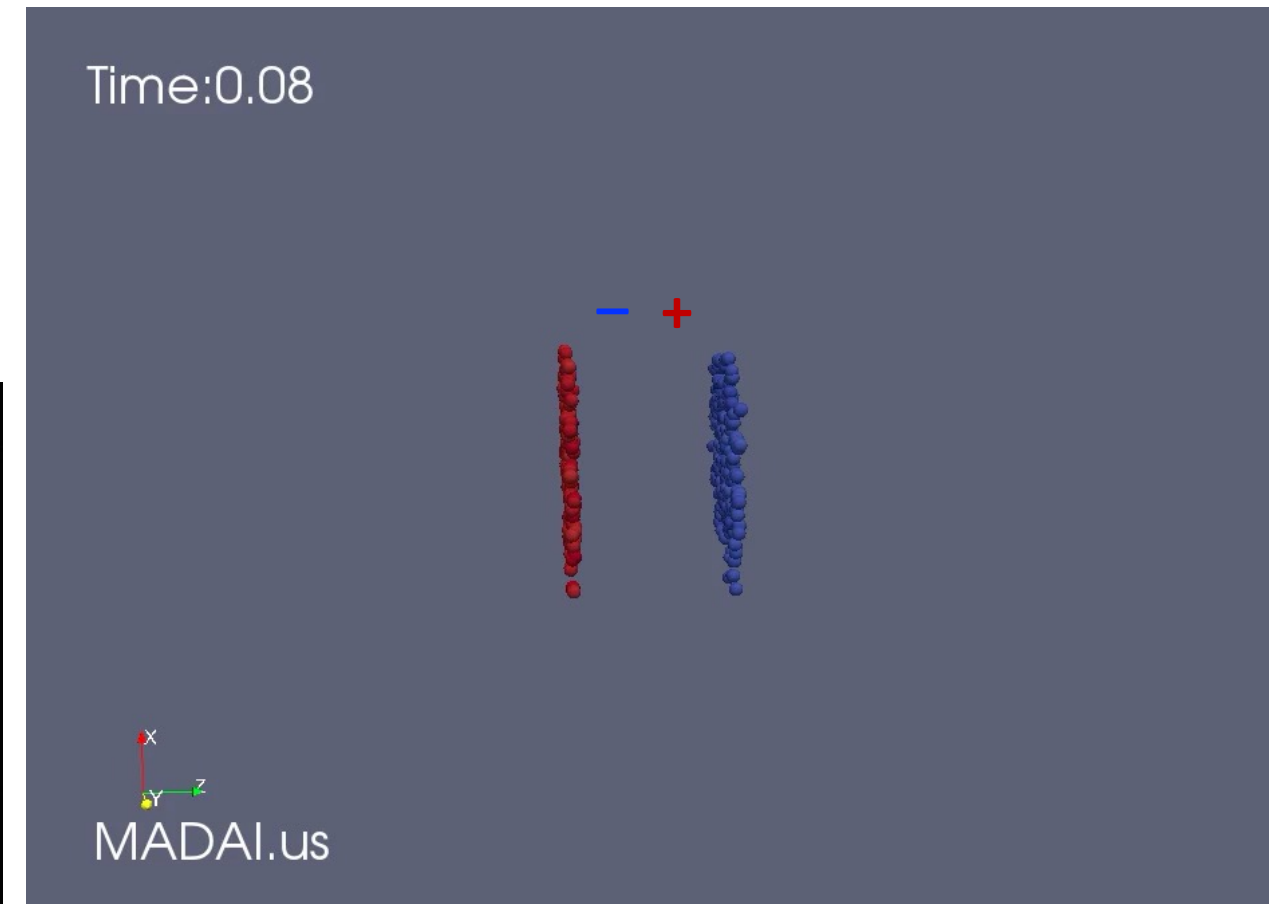
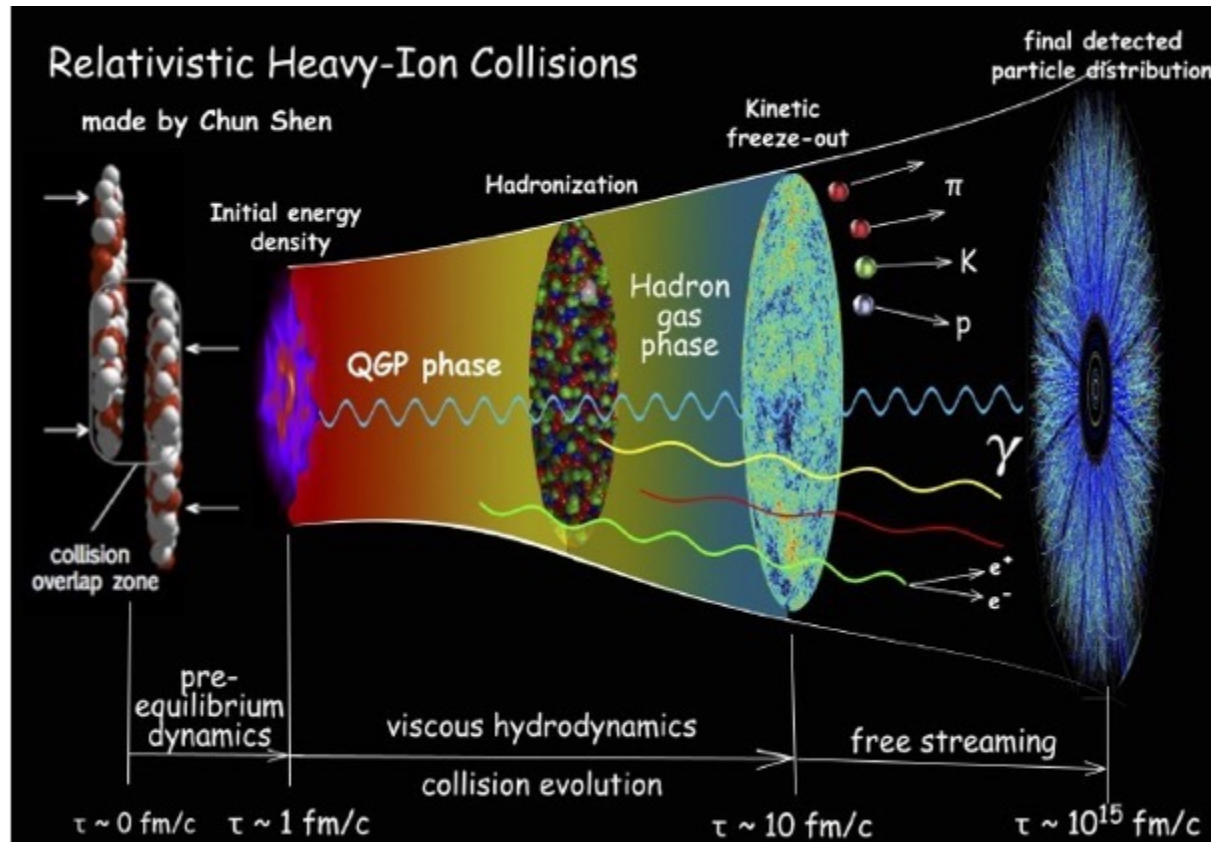
Outline

- Introduction to heavy – ion collisions and the STAR Experiment
- Motivation and Goal
- Analysis Details
- Two – particle Correlation Function
- Balance Function
- Comparison of Data and Model
- Summary and Conclusions

Introduction to Heavy – Ion Collisions

Heavy ions colliding at ultra-relativistic energies instantly produces deconfined Quark-Gluon Plasma (QGP):

- perfect fluid, that is $\sim 10^5$ times hotter than the core of the Sun i.e., ~ 300 MeV (2×10^{12} K).
- Crossover – conversion from QGP to hadron gas phase at ~ 150 MeV and nearly zero baryonic chemical potential.
- QGP forms hadrons (hadronization) after ~ 10 fm/c.
- Finally, hadrons are investigated by our detectors.



- Measuring correlations of the particle directions
 - shows charges move away from each other;
 - i.e., how they "diffuse."

Star Experiment

Collisions measured by the STAR detector:

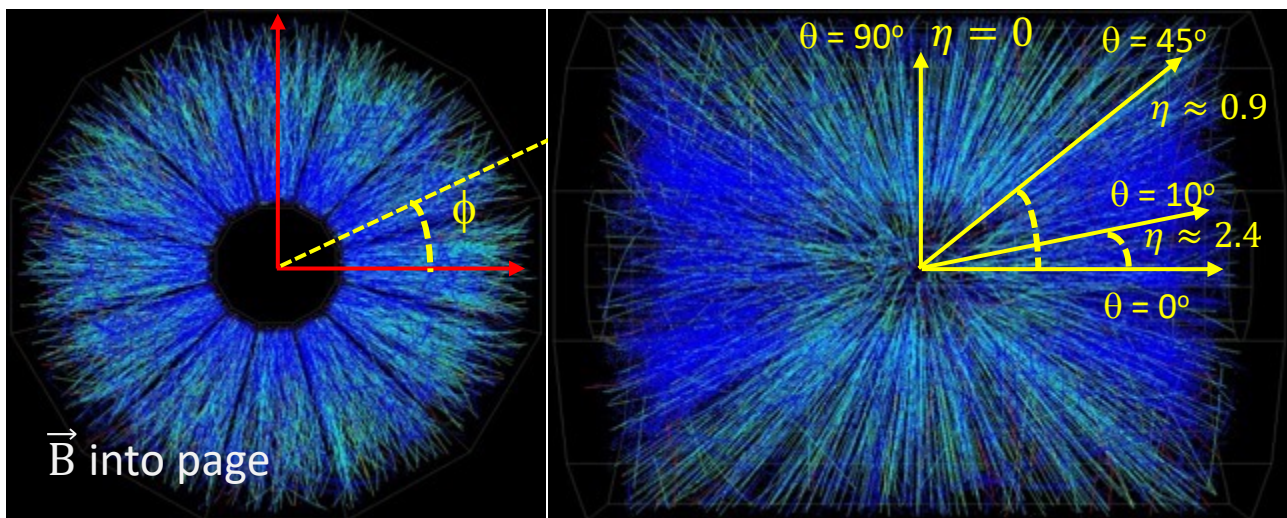
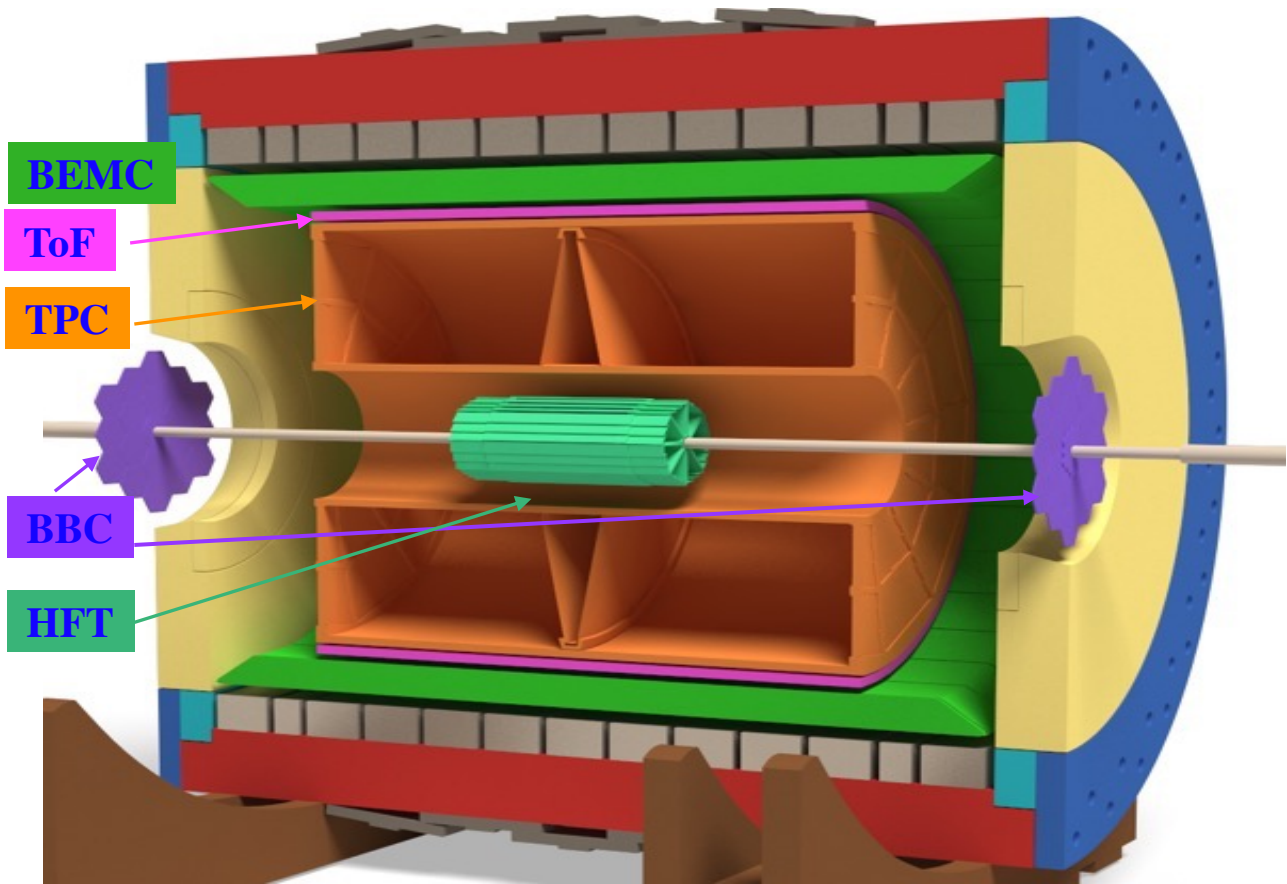
- Time Projection Chamber (**TPC**).
- Time of flight (**ToF**).

TPC measures - momentum of “all” charged tracks in a defined acceptance.

Tracks in TPC are described by:

azimuthal angle, ϕ –transverse

$$\phi = \tan^{-1}(p_y/p_x)$$
$$p_T = \sqrt{p_x^2 + p_y^2}$$



Polar angle θ , along
the beam direction (Z-axis).

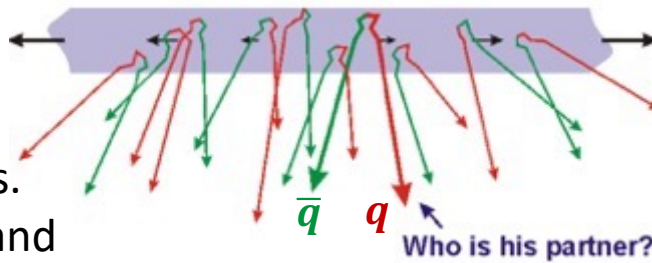
We use (**pseudo**)rapidity instead of θ

$$y = -\frac{1}{2} \ln \frac{(E + p_z)}{(E - p_z)} \quad \eta = -\ln(\tan \frac{\theta}{2})$$

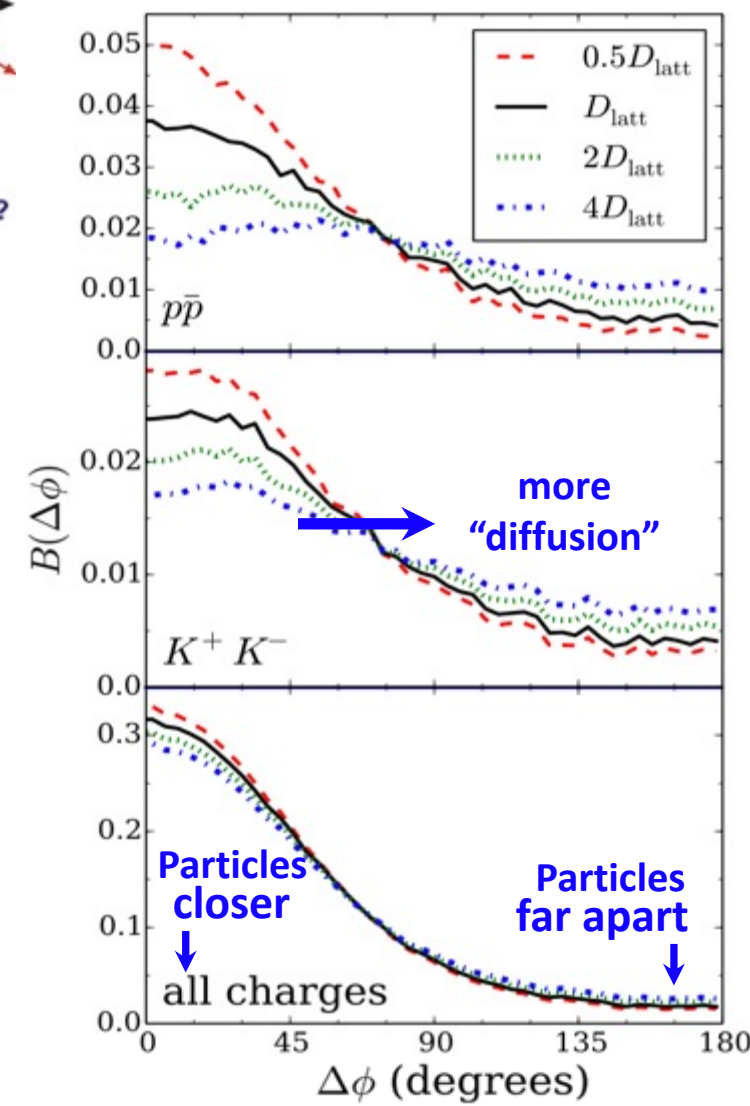
Motivation and Goal

- **Balance function (B_2):**
 - Particles are produced pairs in (q, \bar{q}) .
 - B_2 shows where the charge conserving partner is.
 - B_2 measures – kinematic aspects of production and “diffusion” (i.e., charges moving away from each other).
- **S. Pratt and C. Plumberg’s Model** – diffusion increases when the distribution widens i.e., $\Delta\phi$ increases. Plot shows – balancing charges are moving farther away from each other due to diffusion which changes the shape of B_2 .
- Compare B_2 from data and for events generated from four commonly used models –
 - UrQMD, HIJING, and SMASH – hadronic cascade models.
 - AMPT – hadronic collisions along with quark phase transitions.
- Produced results for B_2 for all possible combinations of π , K , and p i.e., $(\pi, K, p) \otimes (\pi, K, p)$.

$$\begin{pmatrix} \pi\pi & \pi K & \pi p \\ K\pi & KK & kp \\ p\pi & pK & pp \end{pmatrix}$$



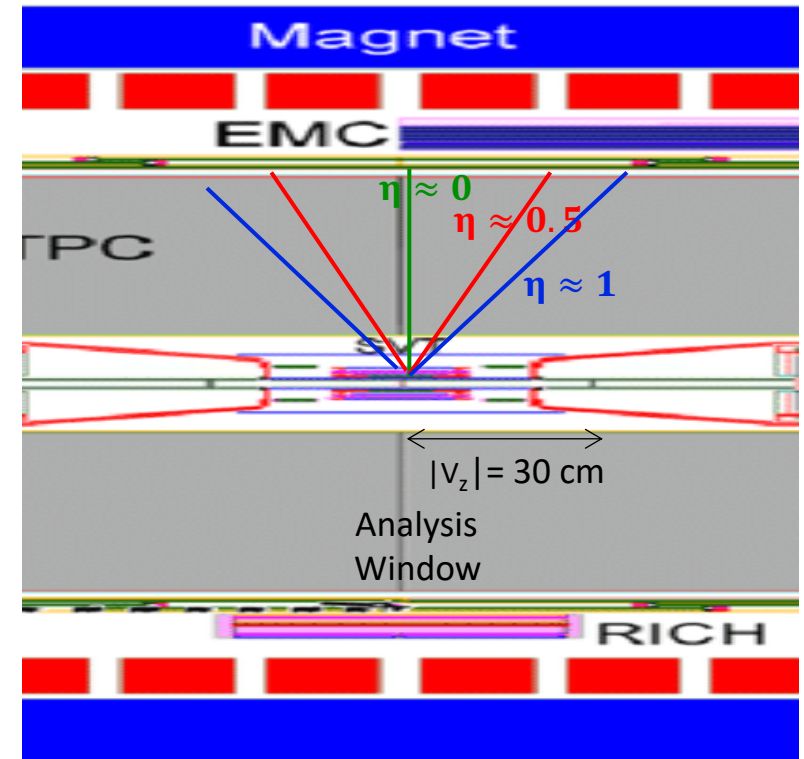
Au+Au , 200 GeV, 0-5% centrality



S. Pratt and C. Plumberg
PRC 102, 044909 (2020)

Analysis details

- Event Selection:
 - Longitudinal distance along beam axis: $|V_z| < 30\text{cm}$.
 - Radial or transverse distance perpendicular to beam axis: $|V_r| < 2\text{ cm}$ respect to the nominal beam position.
- Track Selection:
 - Global distance of closest approach of $< 2\text{ cm}$.
 - No. of hit points fitted to form tracks in the TPC is ≥ 18 .



Correlation functions
are measured inside
this acceptance box.



π^\pm	$0.2 < p_T < 2.0 \text{ GeV}/c$ $0.2 < p_T < 0.6 \text{ GeV}/c$ (TPC)	$p_{\text{tot}} < 1.7 \text{ GeV}/c$ (TOF)	$ y < 0.4$ $ \eta < 0.5$
K^\pm	$0.2 < p_T < 2.0 \text{ GeV}/c$ $0.2 < p_T < 0.6 \text{ GeV}/c$ (TPC)	$p_{\text{tot}} < 1.7 \text{ GeV}/c$ (TOF)	$ y < 0.4$ $ \eta < 0.5$
p^\pm	$0.4 < p_T < 3.0 \text{ GeV}/c$ $0.4 < p_T < 1.0 \text{ GeV}/c$ (TPC)	$p_{\text{tot}} < 2.9 \text{ GeV}/c$ (TOF)	$ y < 0.4$ $ \eta < 0.5$

Analysis details – Data Sets

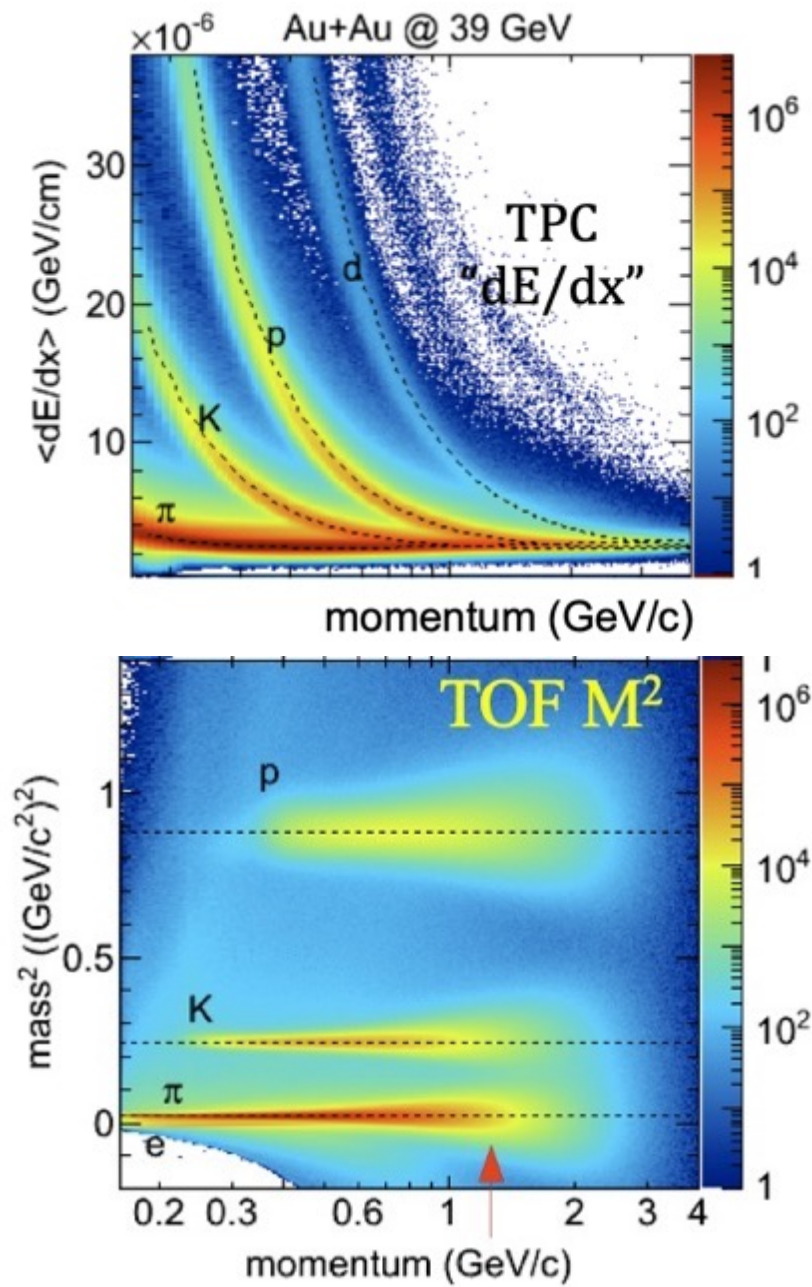
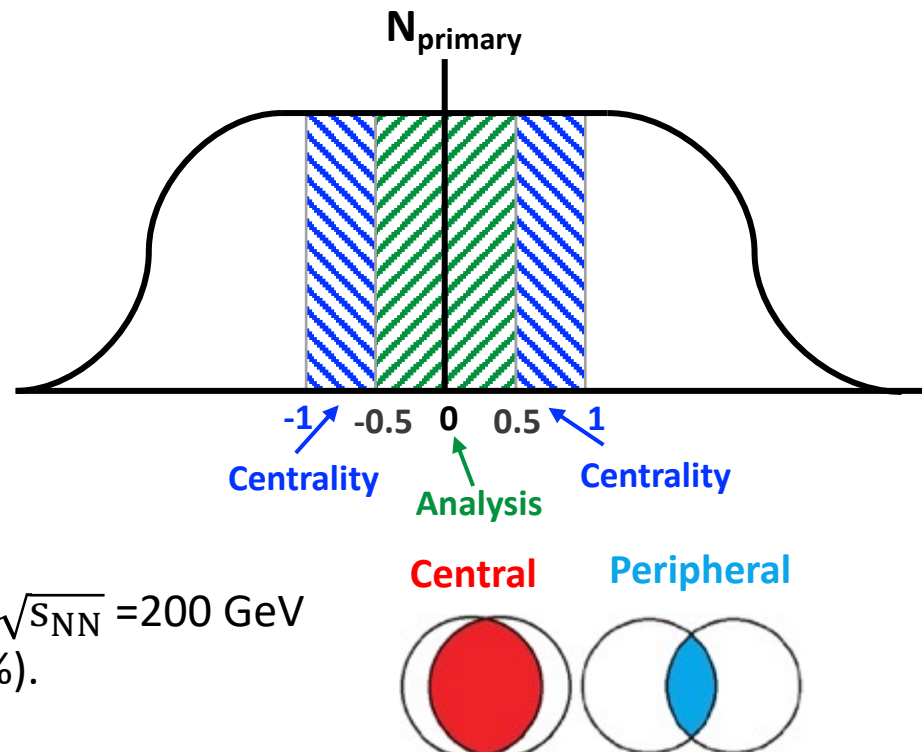
BES-I Dataset – Au+Au

Beam Energy (GeV)	No. of Events (Million)
7.7	4
11.5	12
14.5	20
19.6	36
27	70
39	130
62.4	67
200	45

Entire BES-I dataset analyzed.

This talk focuses on beam energy $\sqrt{s_{NN}} = 200 \text{ GeV}$ of run – 11, central collisions (0-5%).

- Detectors used for particle identification:
 - Time Projection Chamber (TPC).
 - Time of flight detector (ToF).
- Analysis** acceptance uses $(|\eta| < 0.5)$ for all pair types.
- Centrality** definition uses an acceptance of $0.5 < |\eta| < 1$.



Two – particle Correlation Function (R_2)

2-Particle Cumulant or Correlator:

$\rho_2^{ab}(\Delta y, \Delta\phi, \Delta p_{T1})$ density of pairs with particles 'a' and 'b'

$\rho_1^a(y_1, \phi_1, p_{T1}), \rho_1^b(y_1, \phi_1, p_{T1})$, are the single particle densities.

$$C_2^{ab}(\Delta y, \Delta\phi) = \rho_2^{ab}(\Delta y, \Delta\phi) - \rho_1^a \cdot \rho_1^b(\Delta y, \Delta\phi)$$

$$R_2^{a+b-}(\Delta y, \Delta\phi) = \frac{C_2^{ab}(\Delta y, \Delta\phi)}{\rho_1^{a+} \cdot \rho_1^{b-}(\Delta y, \Delta\phi)}$$

R_2 - Corrected for pair-inefficiency called '**crossing**'.

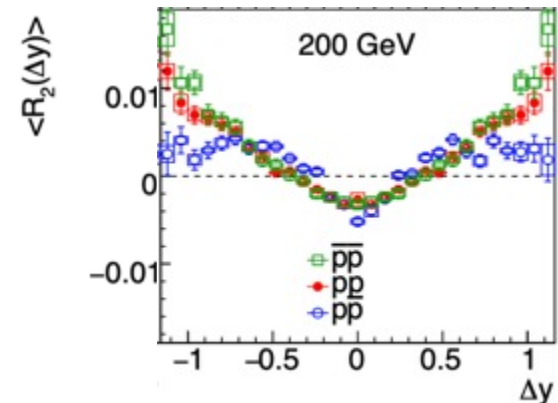
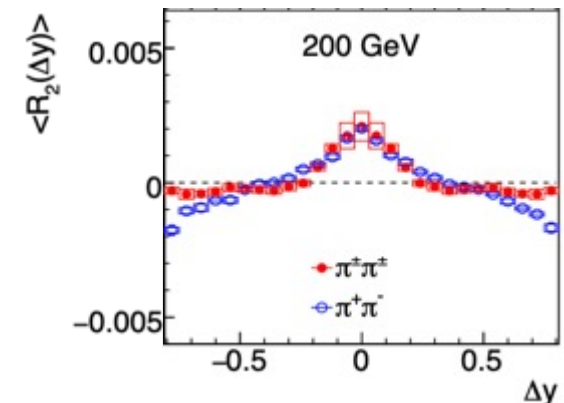
Densities corrected for inefficiencies.

Efficiencies obtained from embedded data.

Denominator filling methods:

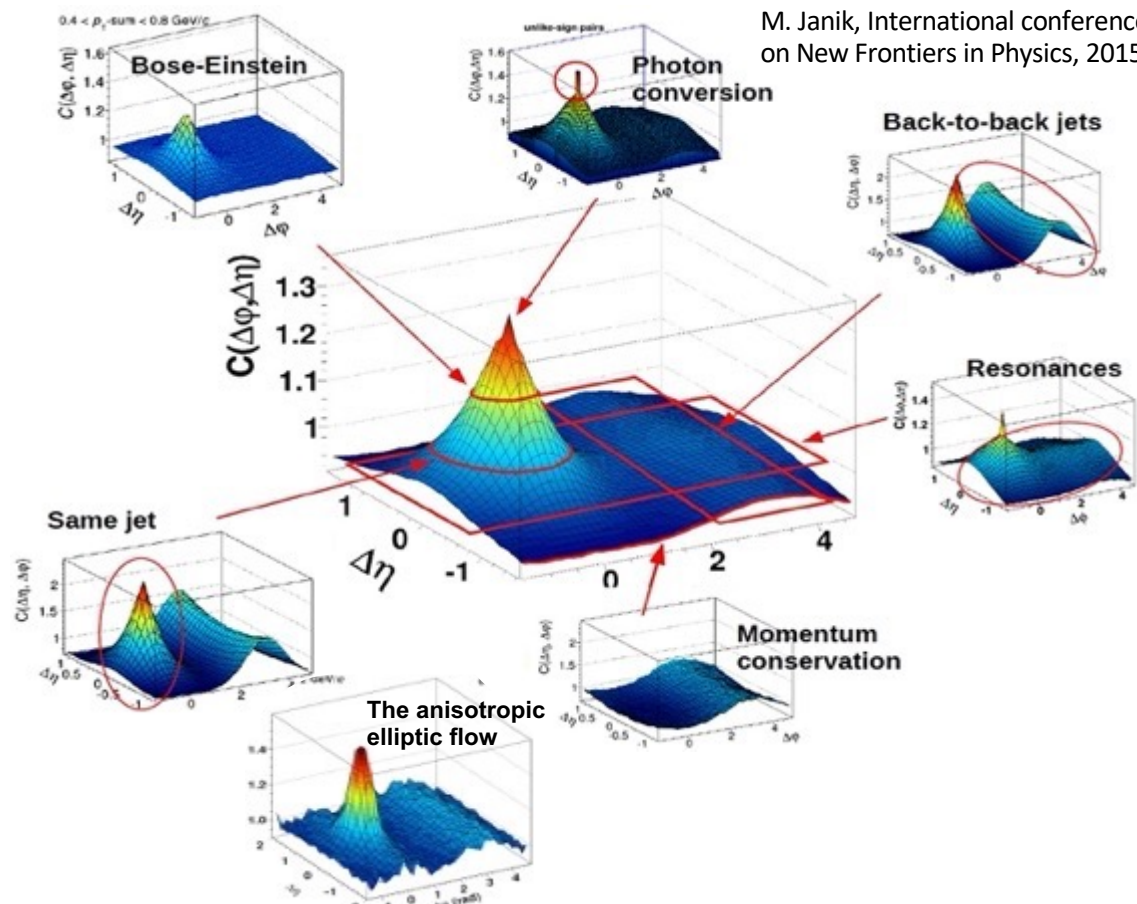
- Convolution: Particle 'a' folded with 'b' in a 6D space
i.e., $(y_1, \phi_1, p_{T1}) \otimes (y_1, \phi_1, p_{T1})$.
- Mixing particles from 2 different but similar events within N_{mix} events.

Mixing approximates convolution as N_{mix} increases.



STAR, Phys. Rev. C 101, 014916 (2020)

M. Janik, International conference on New Frontiers in Physics, 2015



Track crossing correction

- Pairs with overlapping tracks (crossing/merging) are too close for the TPC to resolve them.
- Results in a pair-inefficiency for these particles, causing a crossing "hole" for $(dy, d\phi) \sim 0$.

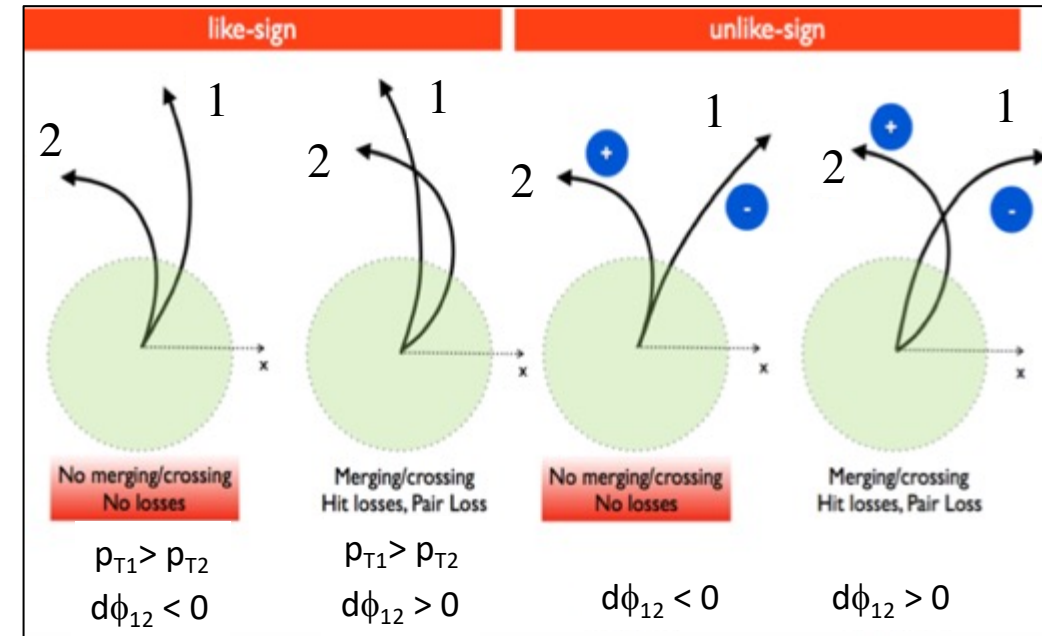
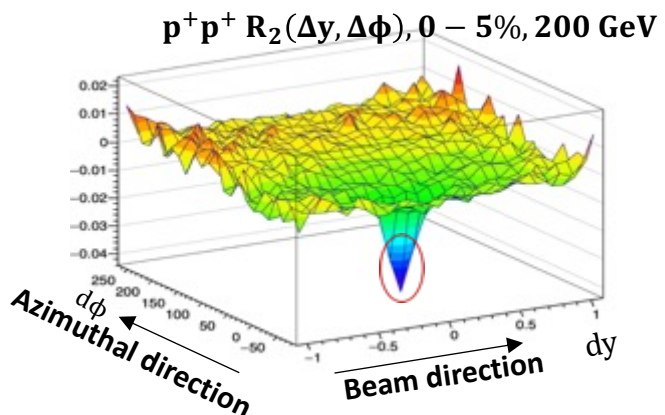
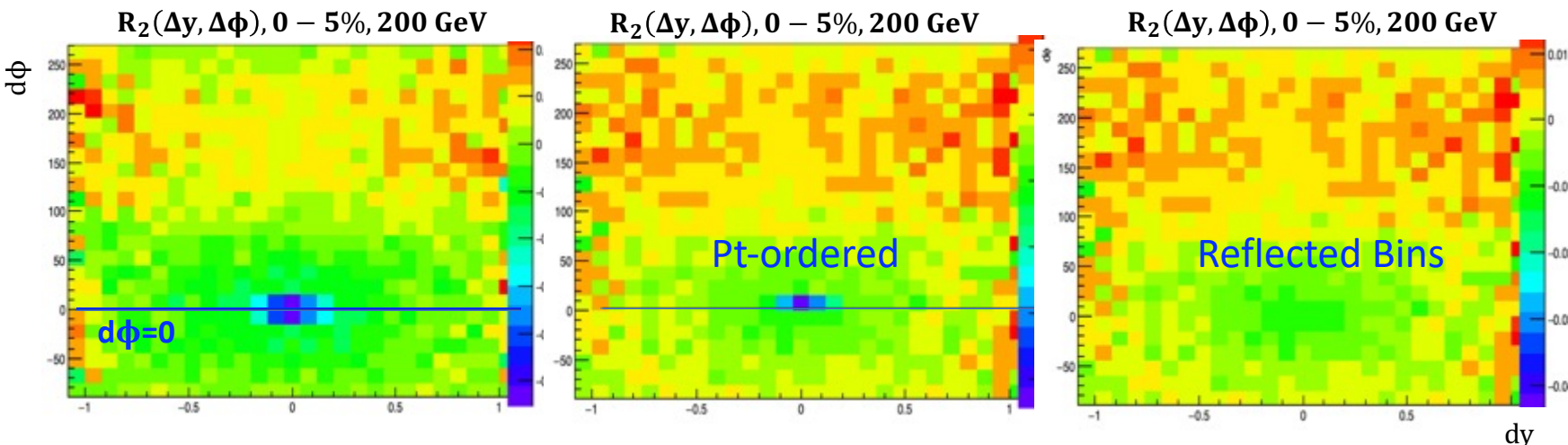


Image Courtesy P. Pujahari

- pt-ordered each pair to move the hole on one side of $d\phi=0$.
- Reflected clean bins as distributions are symmetric about $(dy, d\phi)=0$.
- Finally, symmetrized about $(dy, d\phi)=0$ to undo pt-ordering.

Technique from (Tarini thesis – 01/2011, WSU)



Balance Function (B_2)

Balance Function (B_2)

Balance function B_2 is a multiplicity-weighted two-particle correlation functions.

BF of positive charged particle 1 (a^+):

$$B_2^{a+b}(\Delta y, \Delta\phi) = \frac{\rho_2^{a+b^-}(\Delta y, \Delta\phi)}{\rho_1^{a+}(\Delta y, \Delta\phi)} - \frac{\rho_2^{a+b^+}(\Delta y, \Delta\phi)}{\rho_1^{a+}(\Delta y, \Delta\phi)}$$

$$B_2^{a+b}(\Delta y, \Delta\phi) = N^{b^-} R_2^{a+b^-}(\Delta y, \Delta\phi) - N^{b^+} R_2^{a+b^+}(\Delta y, \Delta\phi)$$

Constants (or prefactors) N^{b^-} and N^{b^+} are efficiency-corrected integrals of $\rho_1^{b^-}$ and $\rho_1^{b^+}$ respectively.

BF of negative charged particle 1 (a^-):

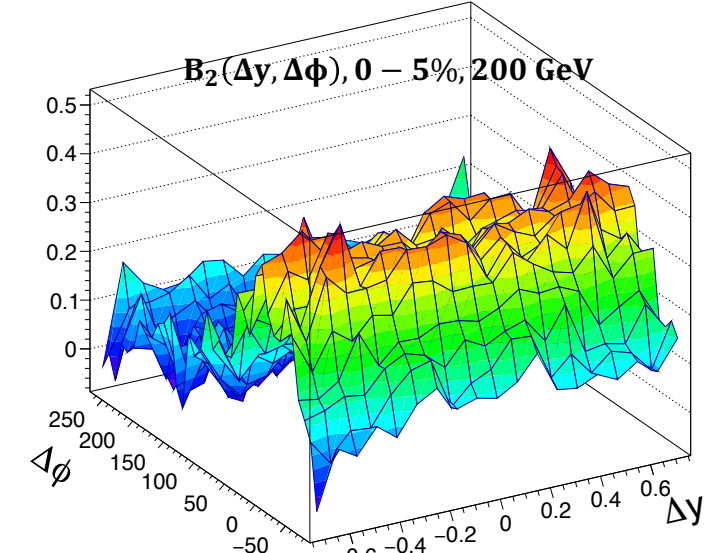
$$B_2^{a-b}(\Delta y, \Delta\phi) = N^{b^+} R_2^{a-b^+}(\Delta y, \Delta\phi) - N^{b^-} R_2^{a-b^-}(\Delta y, \Delta\phi)$$

Charged Balance Function (B_2):

$$B_2 = \frac{B_2^{a+b}(\Delta y, \Delta\phi) + B_2^{a-b}(\Delta y, \Delta\phi)}{2}$$

Two types of pair cuts are applied here:

- **M_{inv}**: rejects pairs from ϕ , K_S , and Λ (and antiparticle) decays using cuts on pair invariant mass (± 10 MeV).
- **Q cut**: rejects pairs with values of the Lorentz-invariant-relative momentum (Q) < 150 MeV. Removes all femtoscopy correlations. STAR, Phys. Rev. C 101, 014916 (2020).



Factorial moment of multiplicity distribution of 'b'

Single particle density: $\langle N^b \rangle = \iint \rho_1^b(\Delta y, \Delta\phi) d(\Delta y) d(\Delta\phi)$

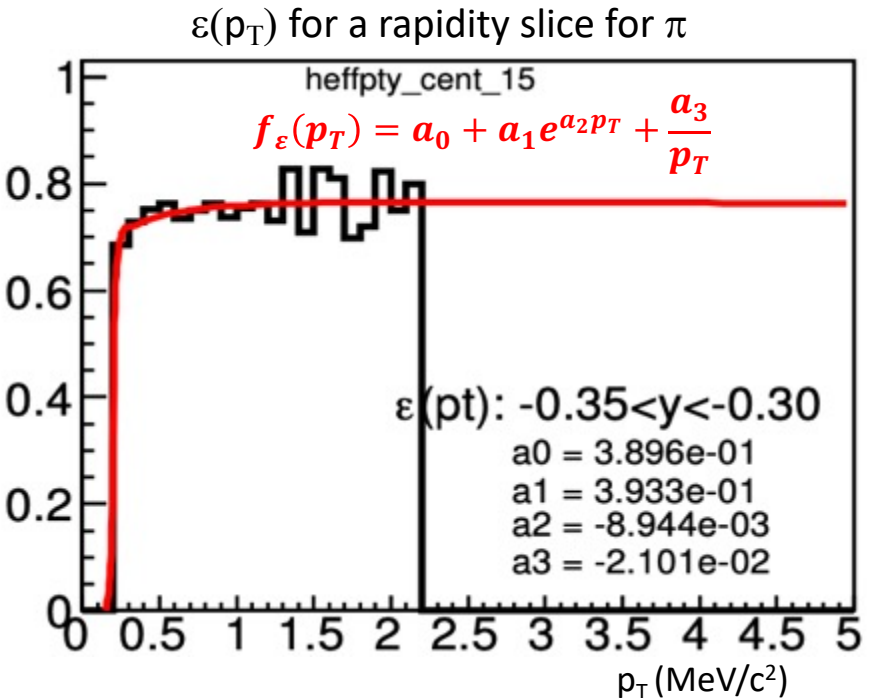
Particle pair density –

Indistinguishable: $\langle N^a(N^a - 1) \rangle = \iint \rho_2^{aa}(\Delta y, \Delta\phi) d(\Delta y) d(\Delta\phi)$

Distinguishable: $\langle N^a N^b \rangle = \iint \rho_2^{ab}(\Delta y, \Delta\phi) d(\Delta y) d(\Delta\phi)$

Efficiency correction from embedded maps

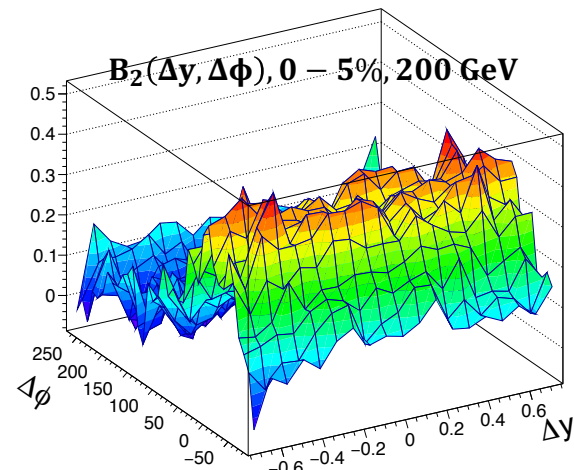
- Inefficiencies are corrected using efficiency maps as functions of (y , p_T) determined by "embedding". These are for every centrality, particle species, charge, and beam energy.
- Fitted values (fit function shown) are used to smooth out the statistical fluctuations.



Integral of Balance Functions

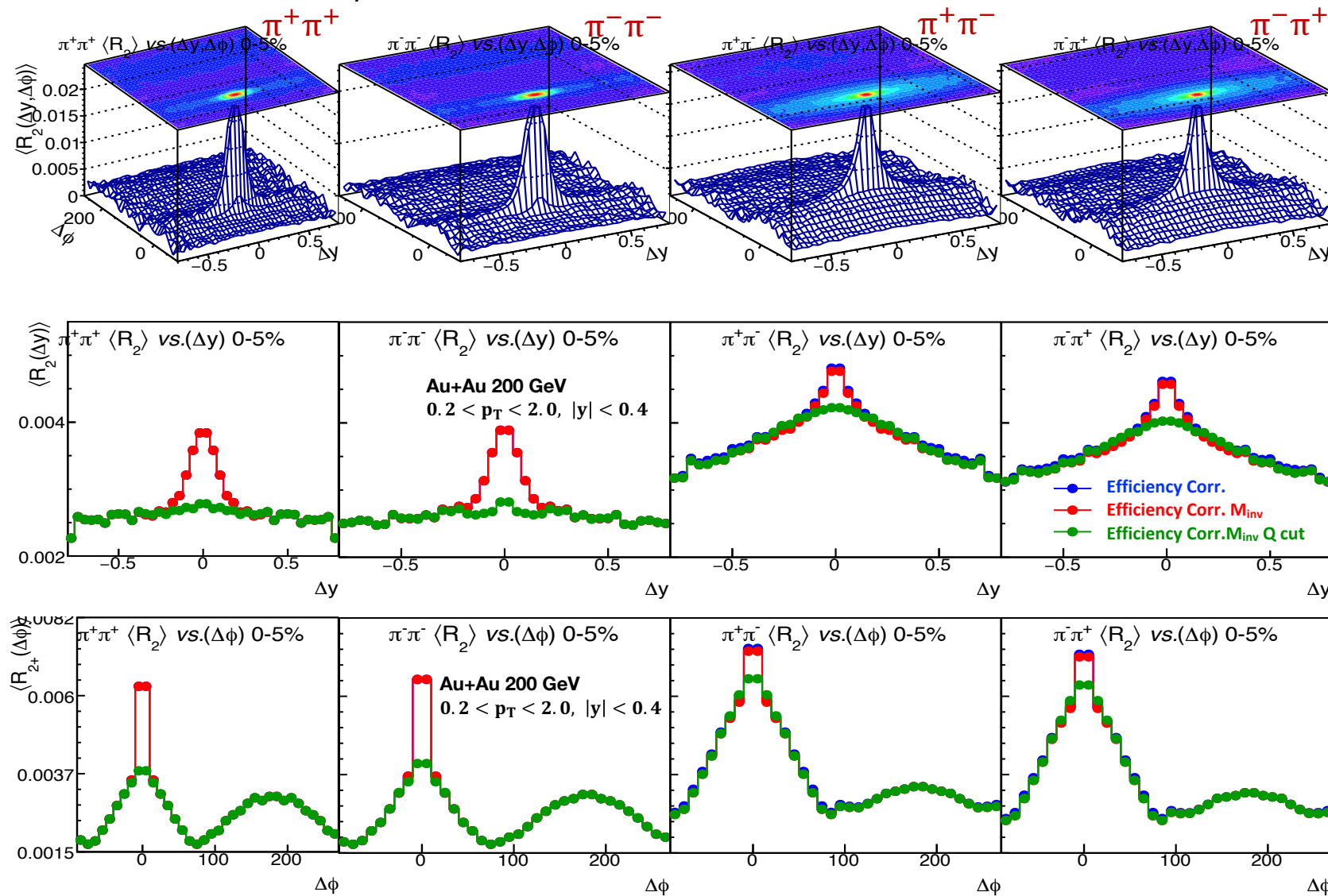
The integral of these B_2 represents the conditional probability of a particle species that is charge balanced with any other particle π , K, and p.

$$I = \iint B_2(dy, d\phi) d(\Delta y) d(\Delta \phi)$$



R_2 for $\pi\pi$ at 0-5% centrality

Explore the effects of the Minv and/or Q cuts on the correlation functions.



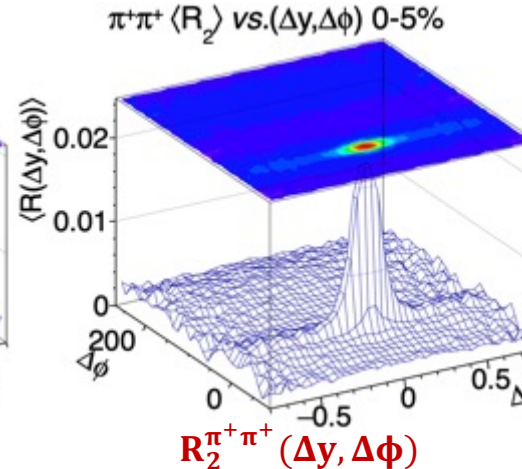
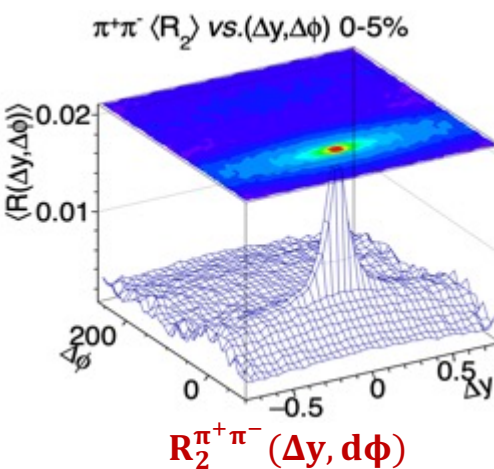
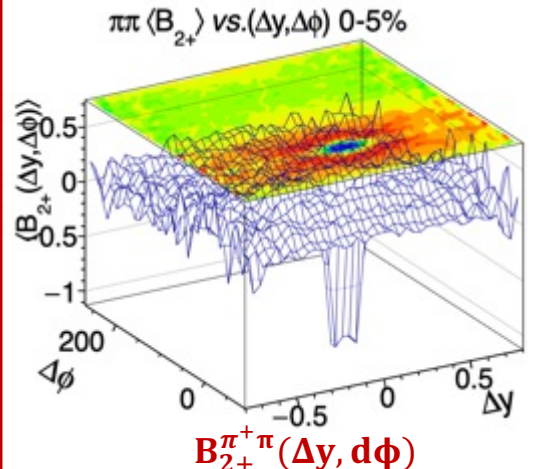
Pion correlations show a peak at $(\Delta y, \Delta\phi) \sim 0$ in both LS and US charge combinations due to femtoscopic correlations.

B₂ from R₂ for ππ 0-5% centrality

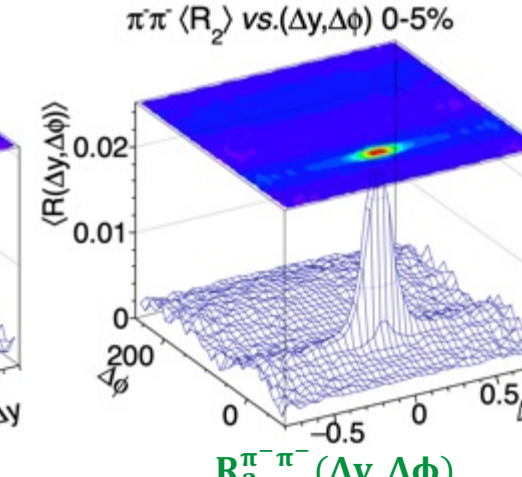
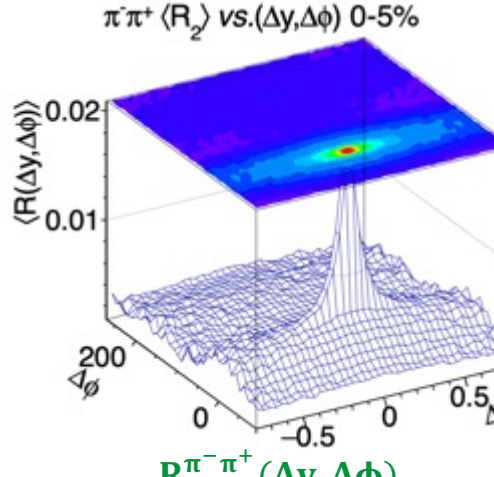
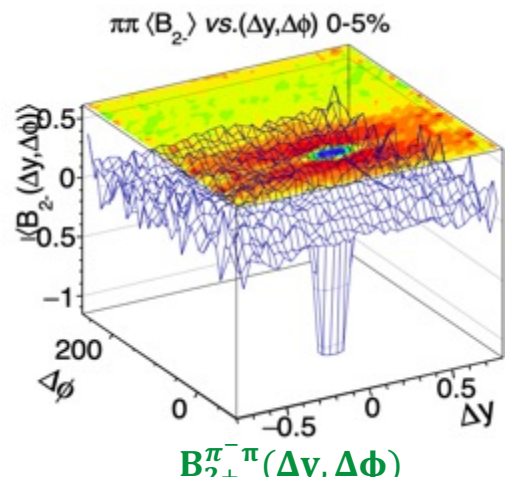
We calculate differential B₂(Δy, Δϕ) using prefactors and R₂(Δy, Δϕ).

a, b → π, π

$$B_2^{\pi^+\pi^-}(\Delta y, \Delta \phi) = N^{\pi^-} R_2^{\pi^+\pi^-}(\Delta y, \Delta \phi) - N^{\pi^+} R_2^{\pi^+\pi^+}(\Delta y, \Delta \phi)$$

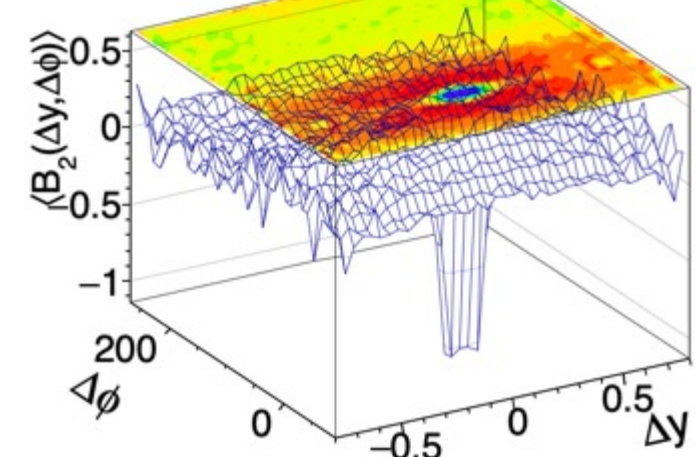


$$B_2^{\pi^-\pi^+}(\Delta y, \Delta \phi) = N^{\pi^+} R_2^{\pi^-\pi^+}(\Delta y, \Delta \phi) - N^{\pi^-} R_2^{\pi^-\pi^-}(\Delta y, \Delta \phi)$$



Au+Au 200 GeV

ππ ⟨B₂⟩ vs.(Δy, Δϕ) 0-5%



$$B_2 = \frac{B_{2+} + B_{2-}}{2}$$

B₂ for ππ at 0-5% centrality

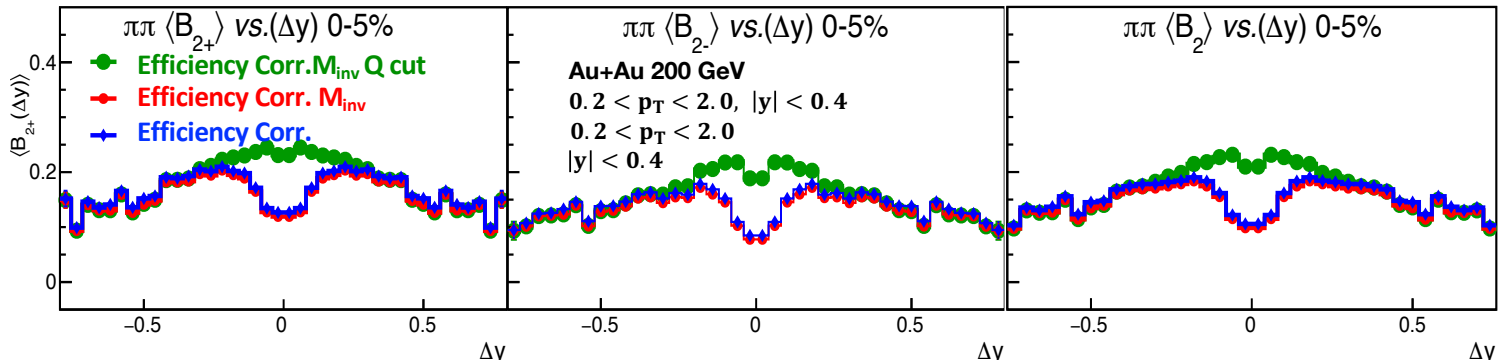
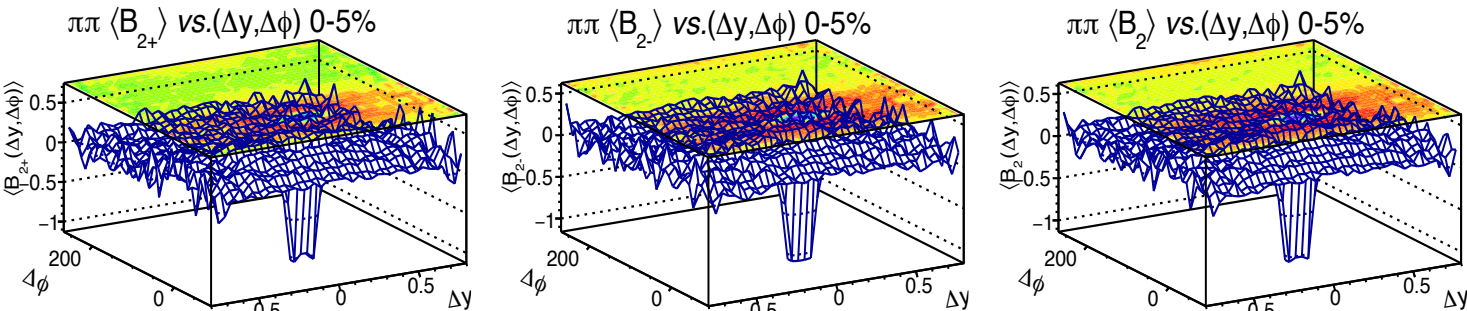
The ridge near $(\Delta y, \Delta\phi) \sim 0$ means the charge conserving partner is nearby.

The observed local decrease of B_2 at $(\Delta y, \Delta\phi) \sim 0$ is due to femtoscopic correlations.

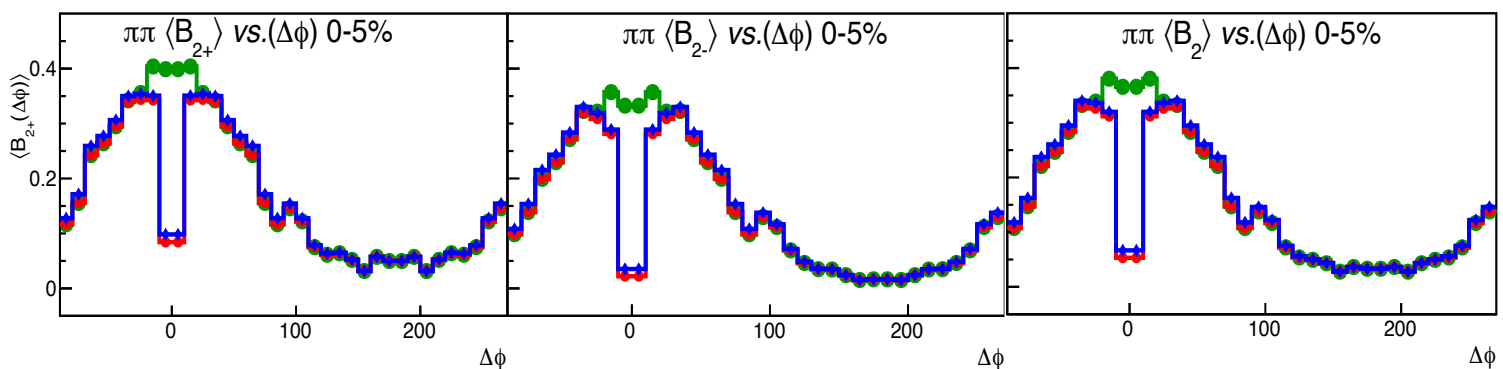
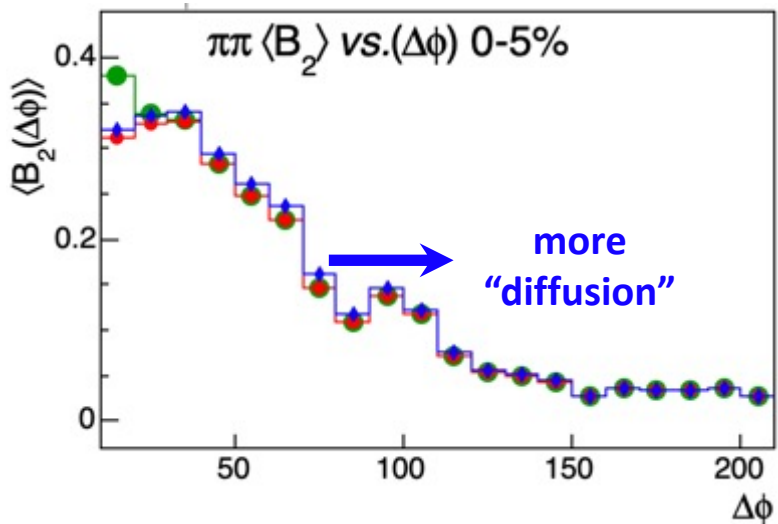
$$B_2^{\pi^+\pi^-}(\Delta y, \Delta\phi) = N^{\pi^-} R_2^{\pi^+\pi^-}(\Delta y, \Delta\phi) - N^{\pi^+} R_2^{\pi^+\pi^+}(\Delta y, \Delta\phi)$$

N^{π^-}, N^{π^+} are comparable.

$R_2^{\pi^+\pi^-}(0, 0) < R_2^{\pi^+\pi^+}(0, 0)$ resulting in a dip in B_{2+}

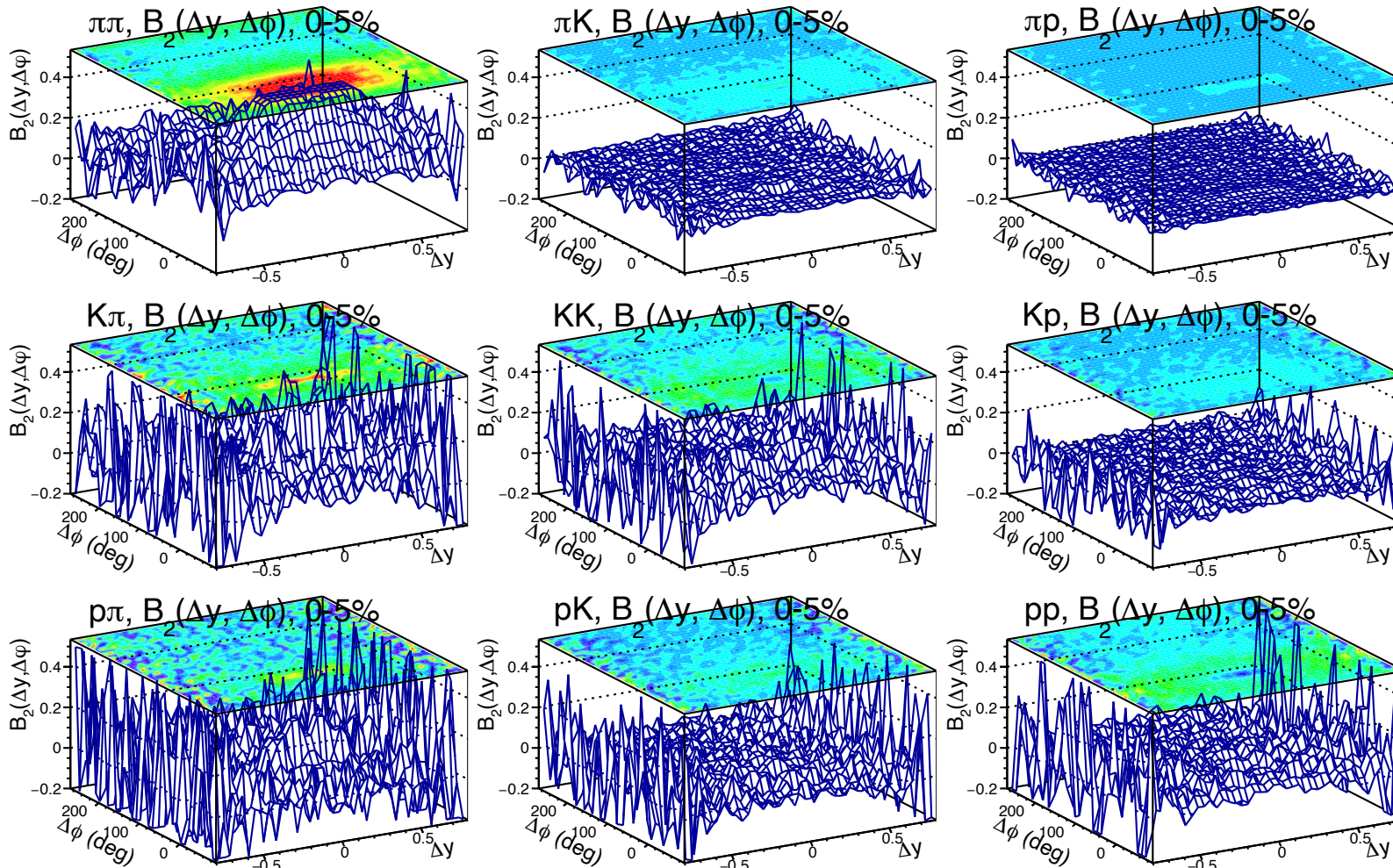


S. Pratt and C. Plumberg's Model



$B_2(\Delta y, \Delta\phi)$ at 0-5% for all species at 200 GeV

All hadron species showing differential $B_2(\Delta y, \Delta\phi)$ in the same scale. Z-axis range: -0.2 to 0.5

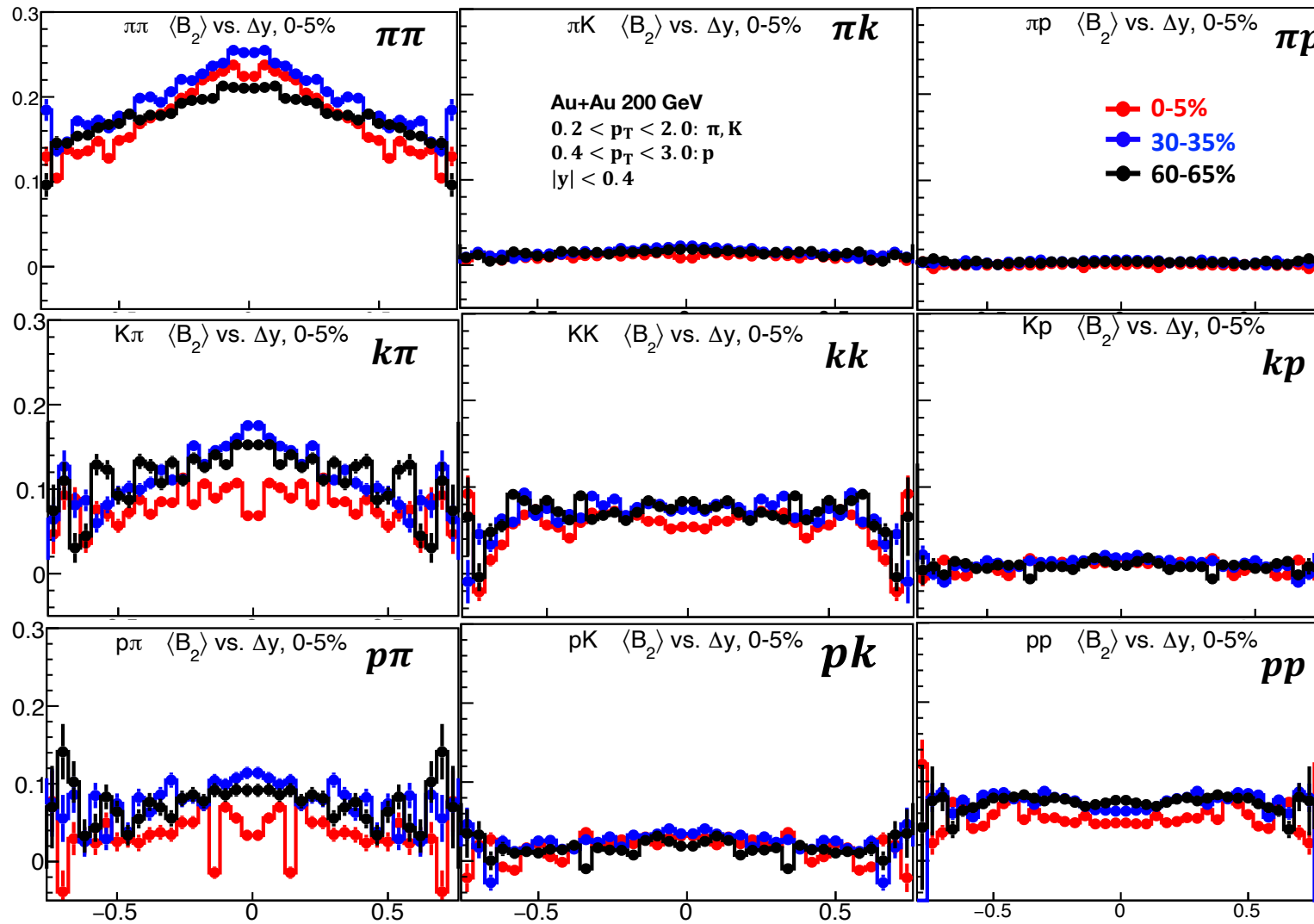


Strongest correlations seen in pions.

All other species combinations have much smaller B_2 values.

$B_2(\Delta y)$ at 0-5%, 30-35%, 60-65% for all species at 200 GeV

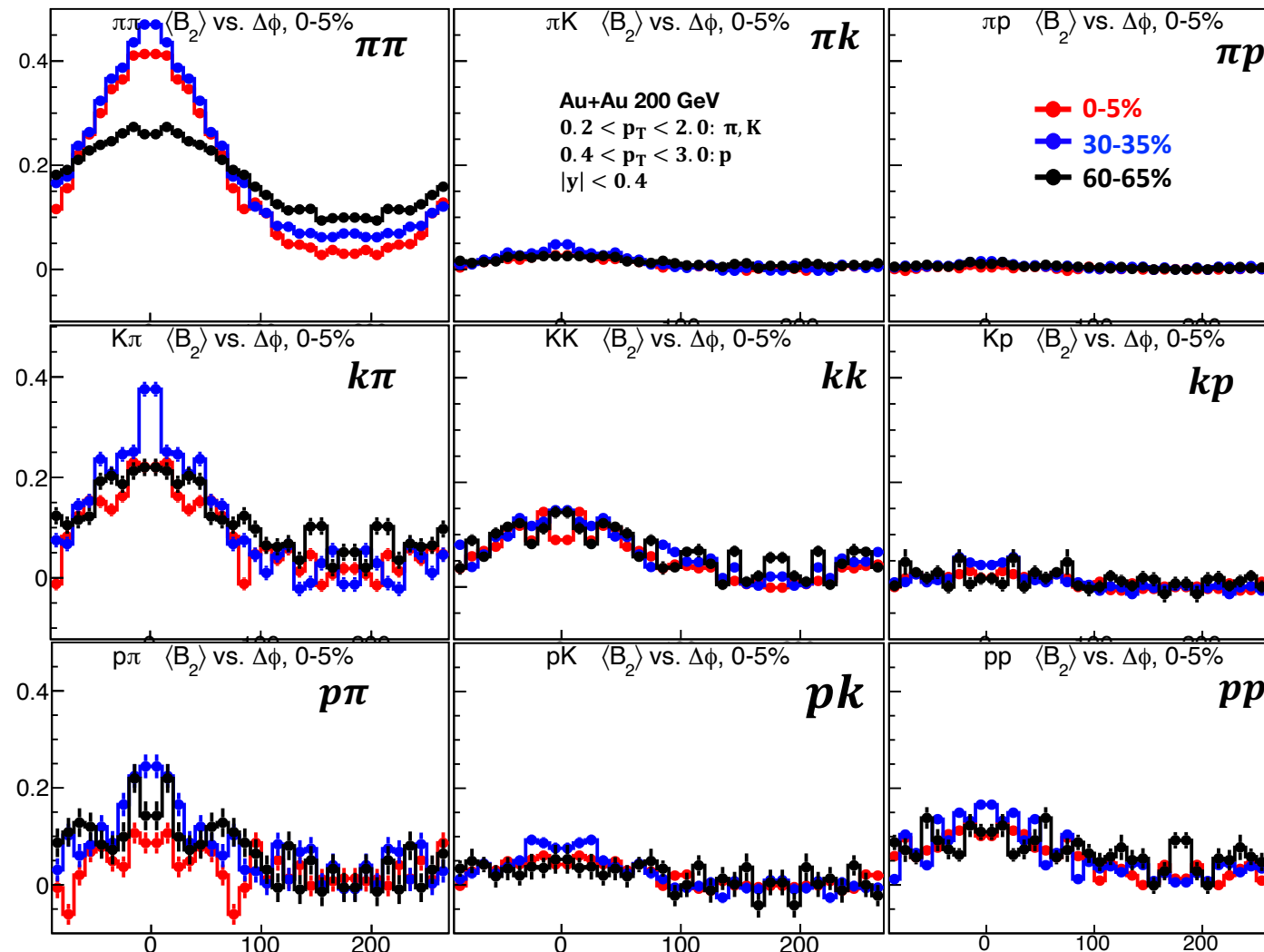
Centrality dependence of relative rapidity projection of B_2 - all in the same scale.



Centrality dependence is quite weak in general.

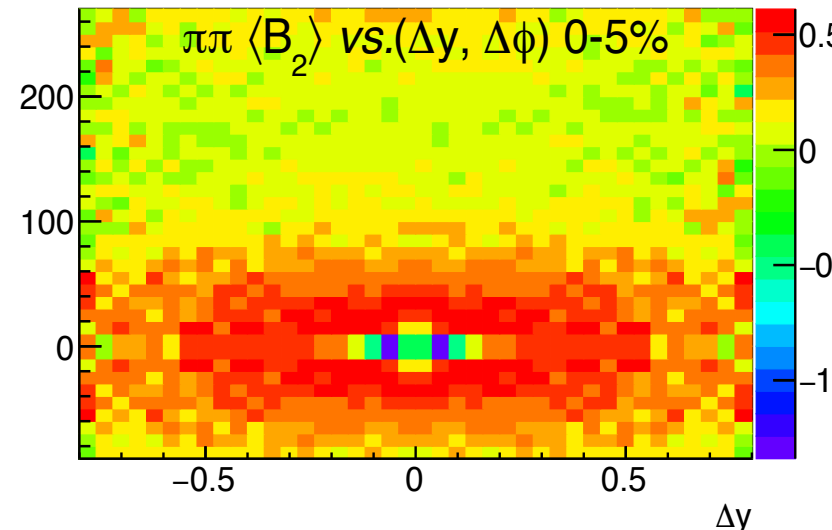
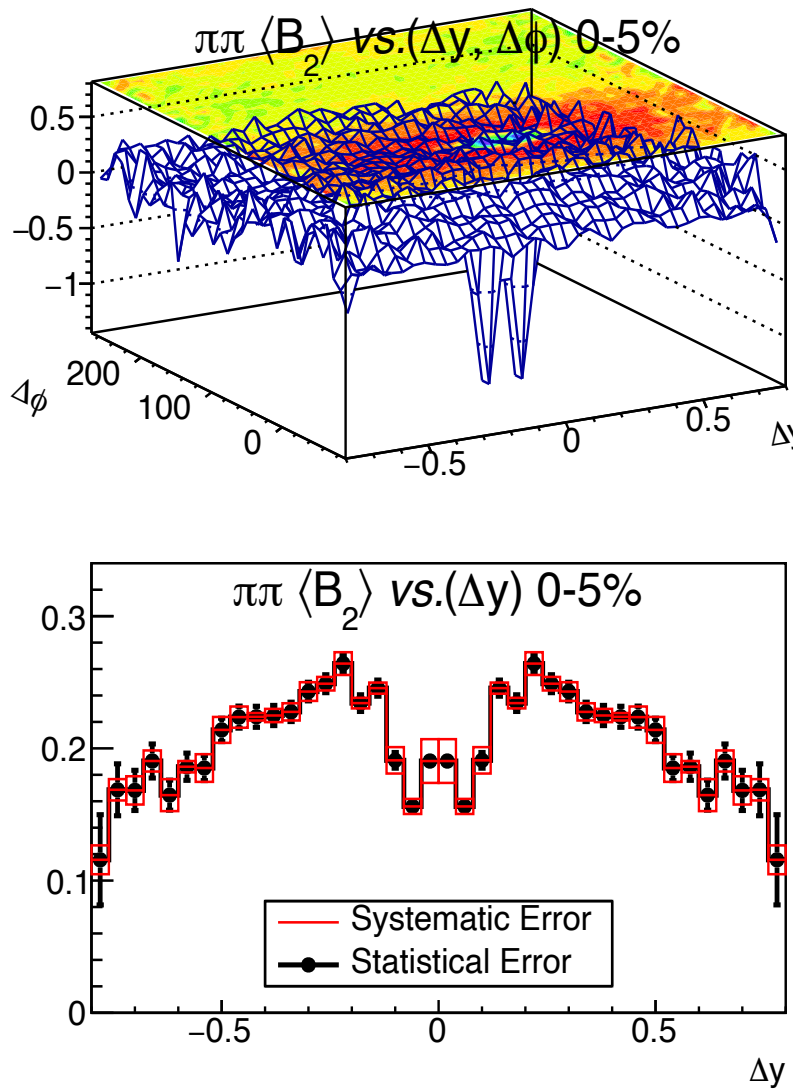
$B_2(\Delta\phi)$ at 0-5%, 30-35%, 60-65% for all species at 200 GeV

Centrality dependence of relative azimuthal projection of B_2 - all in the same scale.



Centrality dependence in species pairs other than $\pi\pi$ is weak in general.

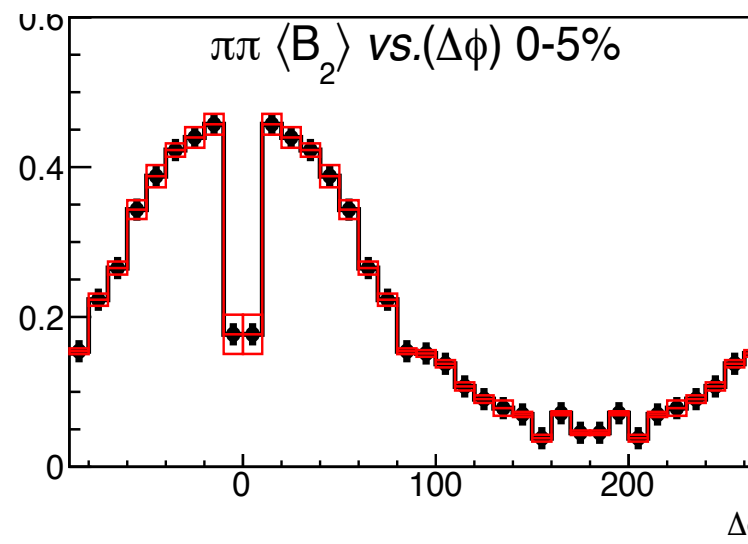
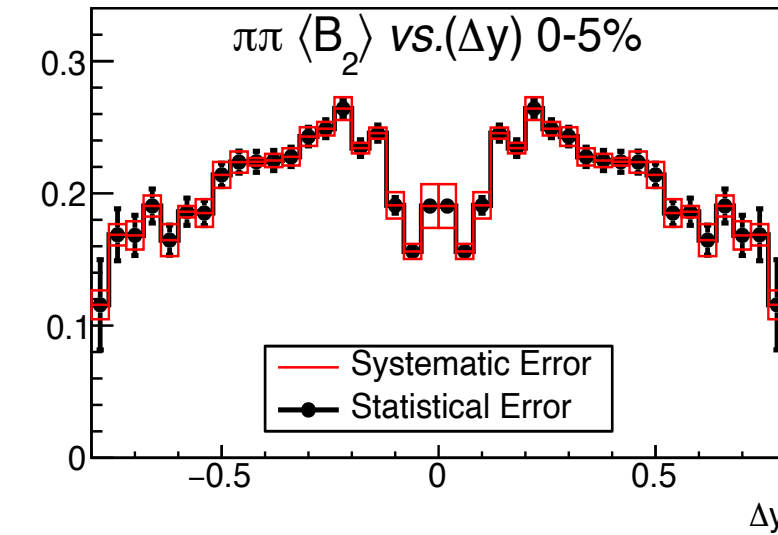
Systematic and Statistical uncertainties of $B_2 - 0 - 5\%$ pions



$N = 4 \times 4$ cutsets: nHits \otimes gDCA				
nHits	14	17	20	23
gDCA (cm)	2.2	1.8	1.4	1

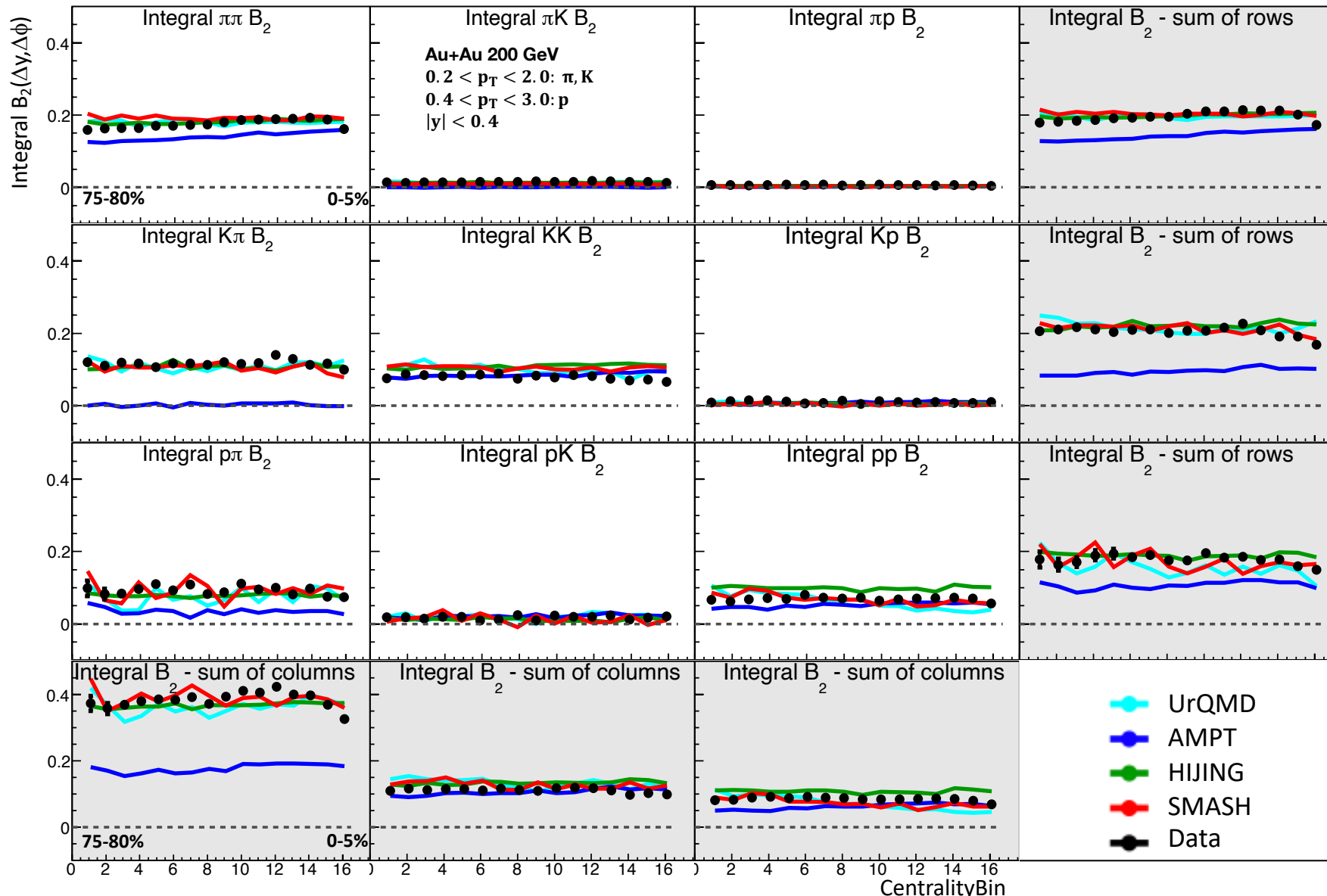
$$\sigma_{sys} = \sqrt{\sum_{i=1}^N \left(\frac{1}{(N-1)} (x_i - \bar{x})^2 \right)}$$

- Efficiency Corrected with no M_{inv} and Q cut.
- Systematic errors are larger than stat errors for central bins near Δy .
- Peripheral bins $|\Delta y| > 0.6$ have systematic errors smaller than statistical.



Comparison of Integrals of B_2 – Model and Data

The integral of these B_2 vs. centrality for all pair types at 200 GeV, both for data and all model is shown.



- The pions have the largest balance functions across the species matrix.
- All 4 models show very little centrality dependence.
- UrQMD, SMASH and HIJING give similar integrals, which are larger than those from AMPT.
- UrQMD, SMASH and HIJING overestimate the KK B_2 integrals.

Summary and outlook.

- We showed charged hadron balance functions, $B_2(\Delta y, \Delta\phi)$, for 200 GeV Au+Au collisions measured by STAR, where all ingredients fully corrected and tested.
- The balance function integrals are significant only for pions.
- The integrals are very weakly dependent on centrality at this beam energy.
- UrQMD, SMASH and HIJING reproduce the experimentally measured $\pi\pi$ B_2 integrals.
- AMPT integrals are too small but is closer to measured data in the case of KK.

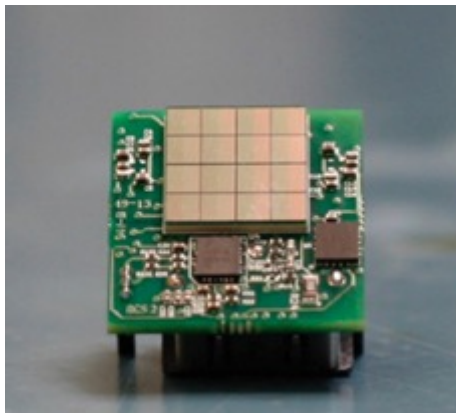
OUTLOOK

- Presently calculating the systematic uncertainties at energies other than 200 GeV.
- The experimental data and embedding efficiencies are in hand for the entire BES-I program, allowing us to form the $3\times 3\times 8$ matrix of balance functions for particle species and beam energy.

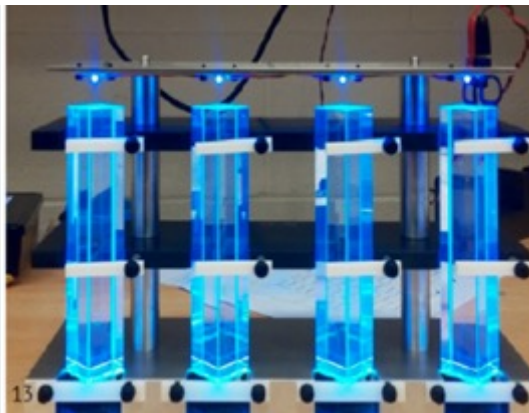
Research Experience – overview of past experiments

Muon g-2 at FNAL – 2015 to 2019 (PostDoc Fellow)

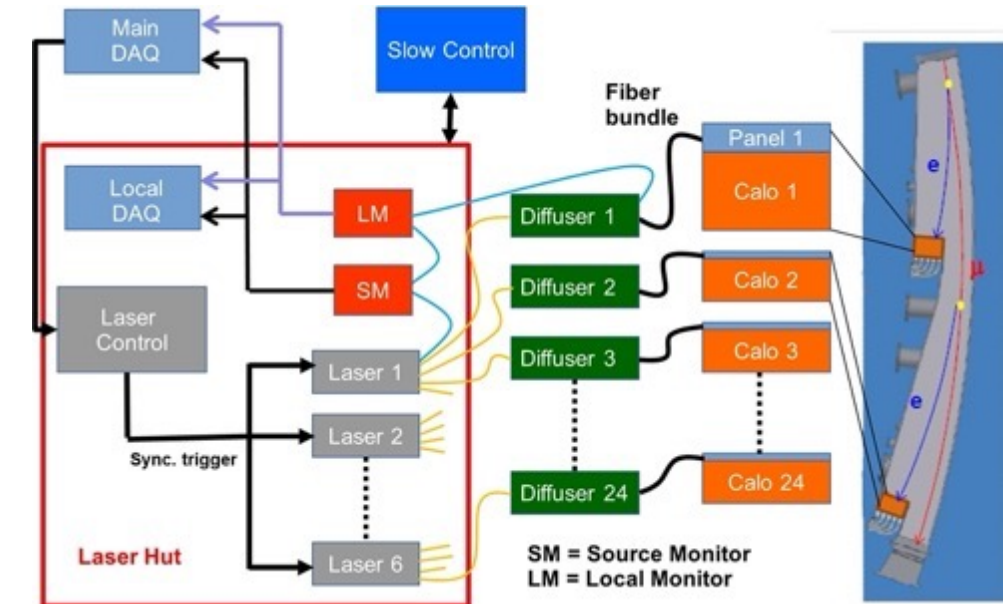
- Precisely finds anomalous magnetic moment of a muon ($a_\mu = \frac{g-2}{2}$) at 0.14 ppm.
- Recent experimental average differs 4.2σ from Standard Model (SM) analyzing $\sim 10^{10}$ events.
- a_μ found indirectly from decay e^+ spectrum ($\mu^+ \rightarrow e^+ + \nu_e + \bar{\nu}_\mu$) – which is measured using 24 calorimeters. Each calorimeter has 9x6 Pb_2F_3 crystals, read-out by SiPM (Si Photo Multiplier)



Si Photo Multiplier



Pb_2F_3 crystals



Worked on **Laser Calibration System** (right fig.) to calibrate and monitor these calorimeter:

- Simulated the optimal conditions for best performance of the calorimeters and laser system.
- Calibrating gains and monitored the gain fluctuations.
- Derived calibration constants and time references for the calorimeters.

Research Experience – overview of past experiments

KLOE2 at LNF (National Lab Frascati, Italy) – 2015 – 2016 (PostDoc Fellow)

- K LOngExperiment2: An $e^+ e^-$ collider experiment at ϕ – meson center of mass energy (1.02 GeV) at DAΦNE.
- Very precise for CP, T and CPT symmetry tests. Used to study SM dynamics, dark matter mediators etc.
- Performed time and energy calibrations of the QCALT (Quadrupole Calorimeters).

MuSun Experiment at PSI – 2010 – 2015 (PhD candidate)

- Muon capture rate in deuterium Λ_d - calibrate a model independent Low Energy Constant (LEC) of any 2-nucleon weak interactions. The μ – capture reaction here: $\mu^- + d \rightarrow n + n + \nu_\mu$
Neutrons emitted – capture neutrons.
- Neutrons emitted from the fusion of $d\mu d$ molecules to He – fusion neutrons which act as a catalyst in the reaction: $d\mu d \rightarrow {}^3 He + n + \mu$.
- Performed the following for these capture neutrons and (Muon Catalyzed Fusion) MCF neutrons:
 - Neutron detector testing, installation, calibration, analysis and software development.
 - Developed Pulse Shape Discrimination (PSD) techniques to distinguish neutrons from gamma rays.
 - Fitted neutron lifetime spectrum.
 - Analytically solutions to find the population of muons in MCF.

Thank you!

Backup

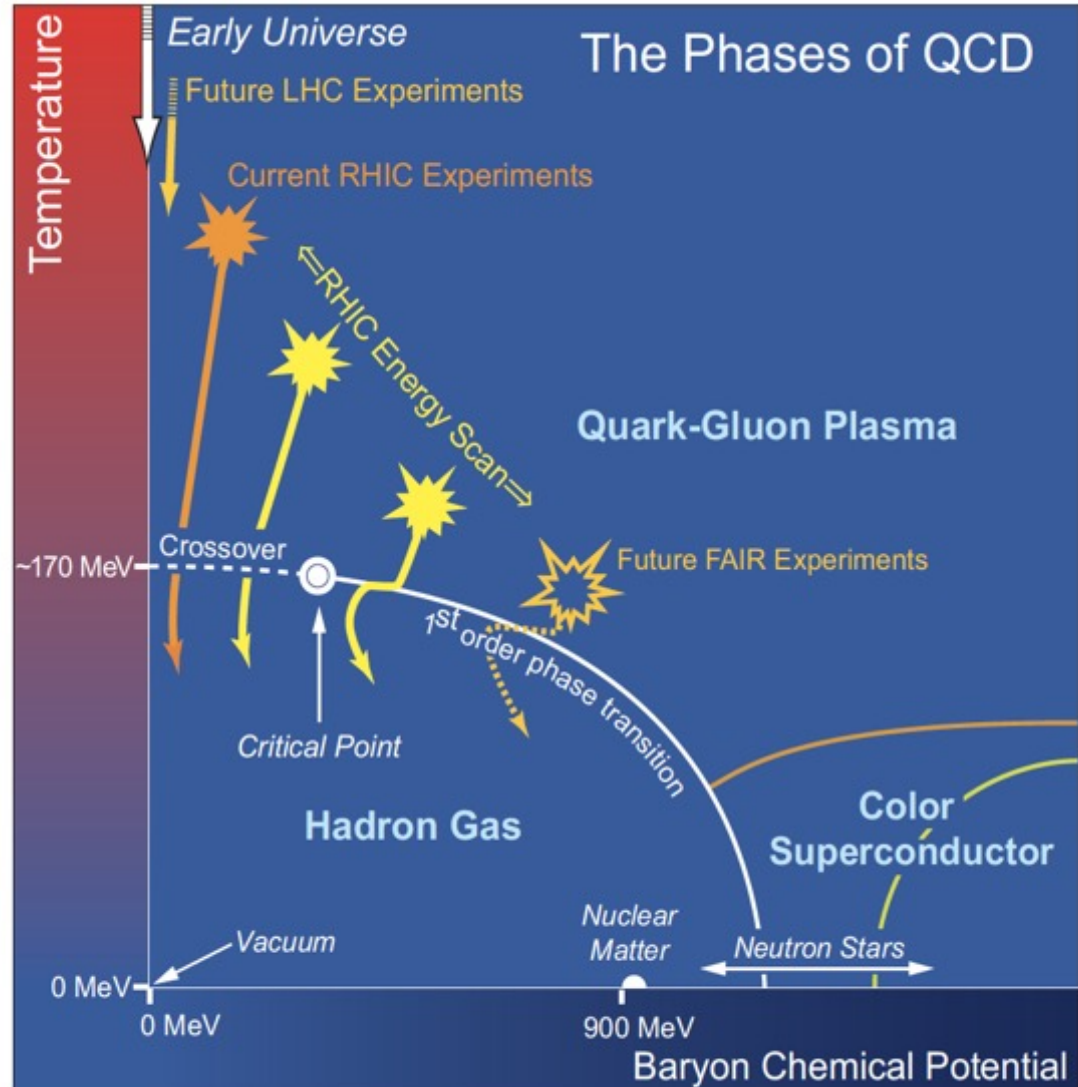
Phase diagram of Nuclear Matter

Physical systems undergo phase transitions when external parameters such as the temperature (T) or baryon chemical potential (μ_B) are varied.

QCD phase diagram studied by varying the collision energies in heavy-ion collision experiments.

From theoretical calculations:

- At low μ_B the phase transition is crossover.
- For higher μ_B , it is expected that there is a critical point beyond which the phase transition is of first order.



Analysis Details – Particle Densities

We count pairs with particles ‘a’ and ‘b’

$\rho_1^a(y_1, \phi_1, p_{T1})$ and $\rho_1^b(y_1, \phi_1, p_{T1})$, are the single particle densities of species ‘a’ and ‘b’.

ρ_1 – counting particles:

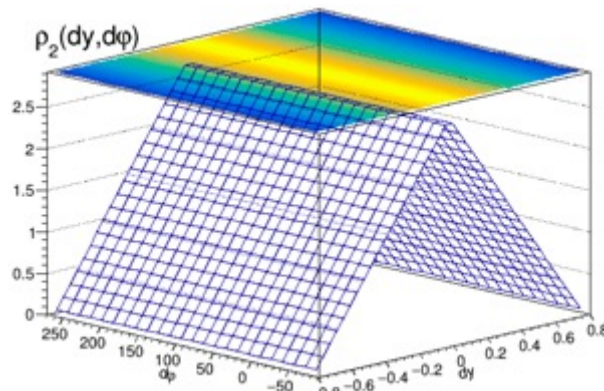
Loop over N tracks in the acceptance

$$\rho_1(y) \rightarrow \text{Fill} \left(y_1, \text{weight}=1.0/\varepsilon(y_1, \phi_1, p_{T1}) \right)$$

end loop

after processing N events, $\rho_1 /= \text{Nevents}$

$\varepsilon(y_1, \phi_1, p_{T1})$: the single-particle efficiency obtained from embedding.



Forming the densities (ρ_2 – counting pairs):

in each event with N tracks in the acceptance

i-loop over tracks in this event

j-loop over tracks in this event

if (i==j) continue

$$dy = y[i] - y[j];$$

$$d\phi = \phi[i] - \phi[j];$$

$$\rho_2 \rightarrow \text{Fill}(dy, d\phi, \frac{1}{\varepsilon(y[i], \phi[i], p_T[i]) * \varepsilon(y[j], \phi[j], p_T[j])})$$

After processing N events, $\rho_2 /= \text{Nevents}$

Two types of pair cuts can be applied in the pair loop above:

- **M_{inv}**: rejects pairs from ϕ , K_S , and Λ (and antiparticle) decays using cuts on pair invariant mass (± 10 MeV).
- **Q cut**: rejects pairs with values of the Lorentz-invariant-relative momentum (Q) < 150 MeV. Removes all femtoscopic correlations.
STAR, Phys. Rev. C 101, 014916 (2020).

Analysis Details – Mixing vs. Convolution

$$R_2^{a+b^-}(\Delta y, \Delta\phi) = \frac{\rho_2^{a+b^-}(\Delta y, \Delta\phi)}{\rho_1^{a+} \cdot \rho_1^{b^-}(\Delta y, \Delta\phi)} - 1$$

Denominator of $R_2^{a+b^-}$ formed by **mixing** or convolution

Mixing with $N_{\text{mix}} = 5$

i-th particle event ids = {1, 2, 3,N}

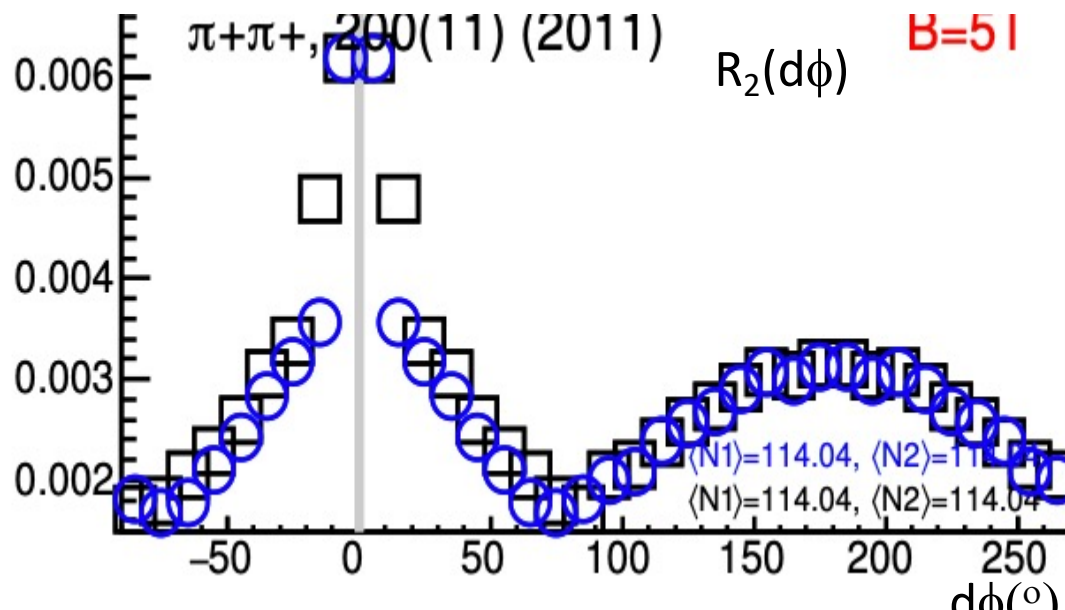
j-th particle event ids = {1, 2, 3, 4, 5, 6, 7, 8, 9, 10,,N}}

Convolution

i-th particle event ids = {1, 2, 3,N}

j-th particle event ids = {1, 2, 3,N}

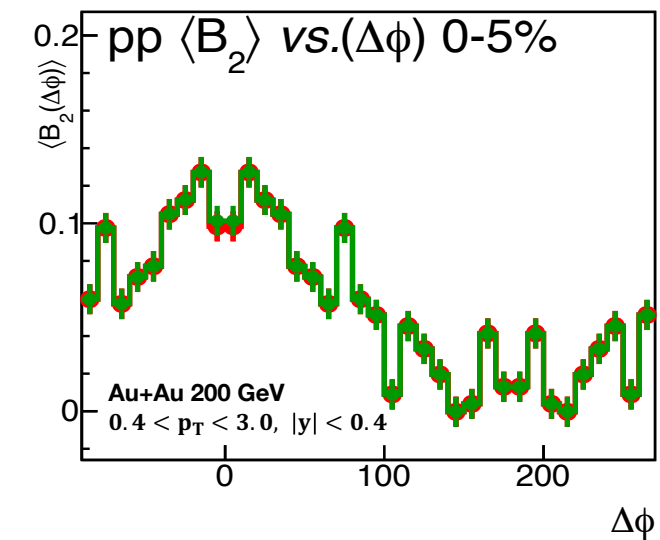
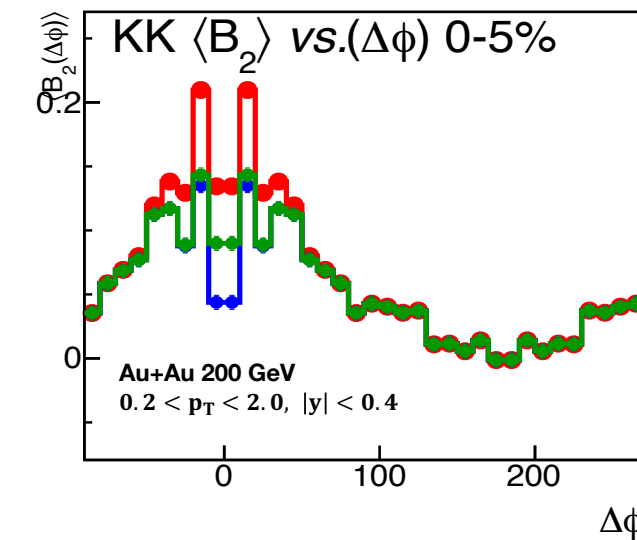
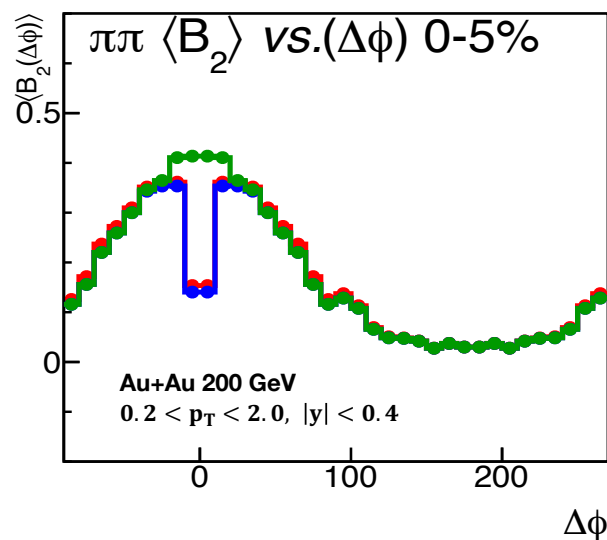
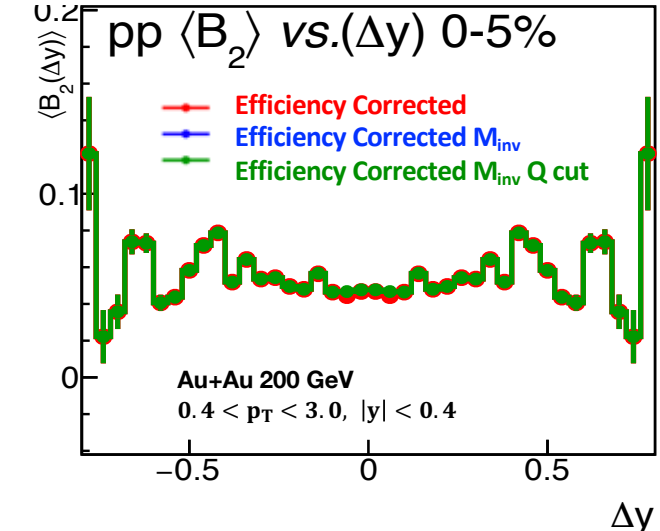
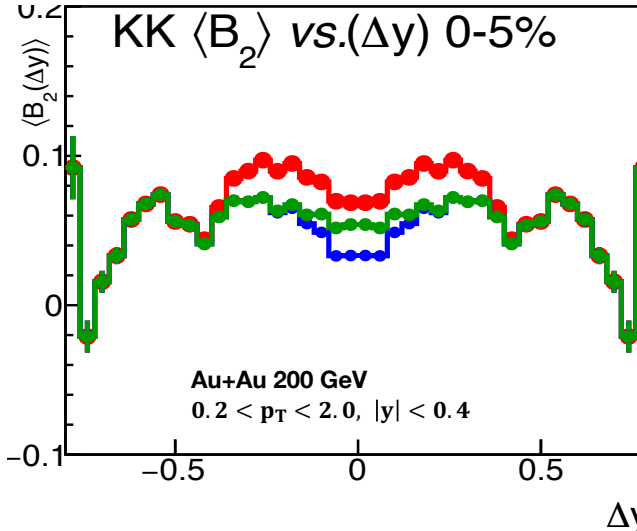
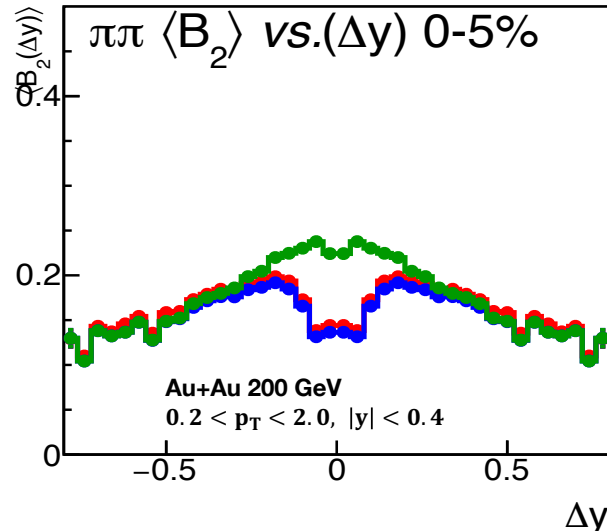
$$\rho_1^{a+}(y_1, \varphi_1, p_T)_1 \otimes \rho_1^{b^-}(y_1, \varphi_1, p_T)_1$$



Comparing $R_2(d\phi)$ mixing ($N_{\text{mix}} = 40$) and convolution for Au+Au collisions Run-11 at 200 GeV at 0-5% centrality. Show good agreement. As N_{mix} increases mixing and convolution agree more.

All identical species 0-5% centrality

Comparison of the effect of M_{inv} and Q cuts for all identical species.



Significant femtoscopic correlations in pions observed. Significant ϕ decays in kaons seen.

$B_2(\Delta y)$ for πK at 0-5% centrality

An example of B_2 of **mixed species pair πK** .

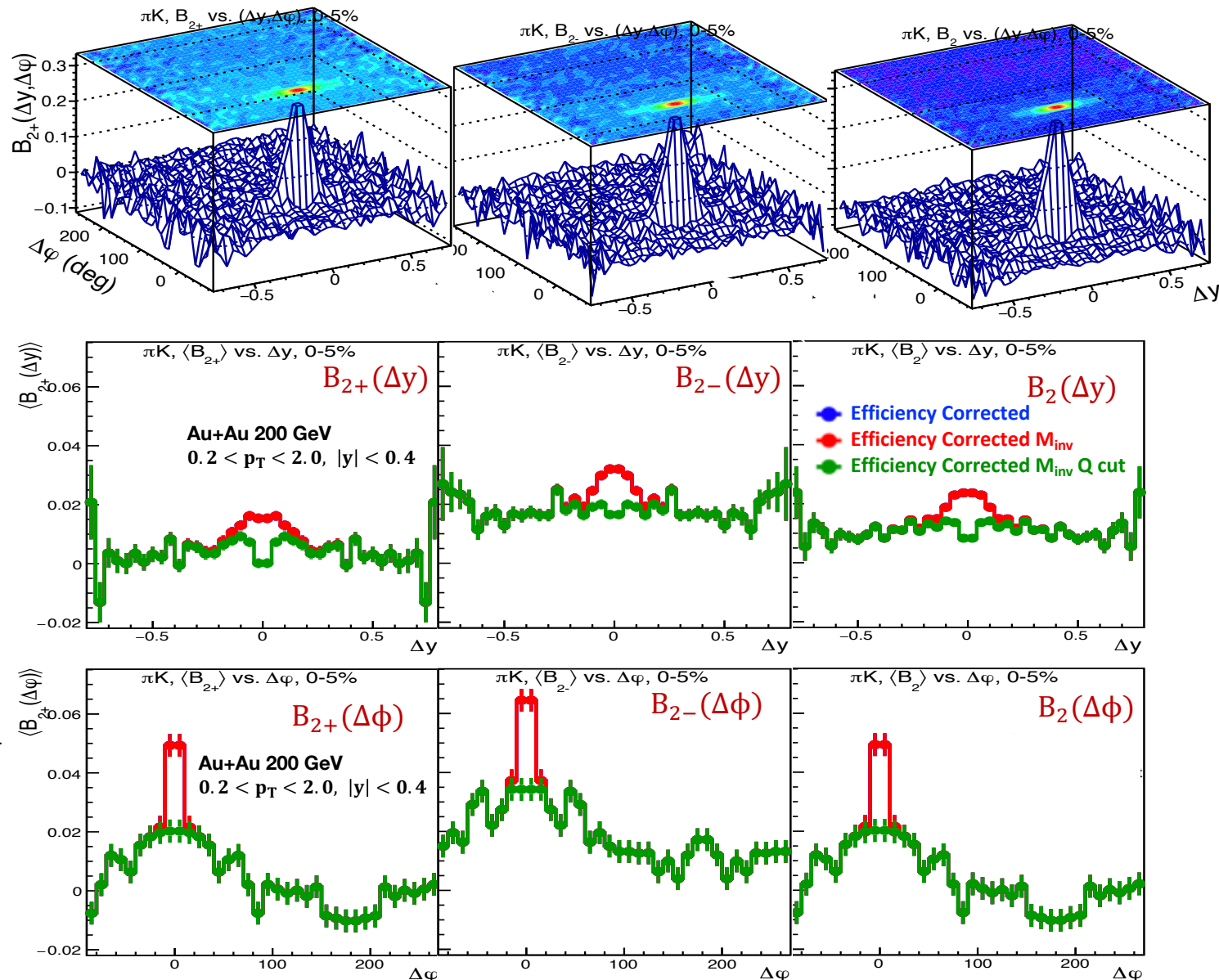
$$B_2^{a+b}(\Delta y, \Delta\phi) = N^{b^-} R_2^{a+b^-}(\Delta y, \Delta\phi) - N^{b^+} R_2^{a+b^+}(\Delta y, \Delta\phi)$$

$a, b \rightarrow \pi, K$

$$B_2^{\pi^+ K}(\Delta y, \Delta\phi) = N^{K^-} R_2^{\pi^+ K^-}(\Delta y, \Delta\phi) - N^{K^+} R_2^{\pi^+ K^+}(\Delta y, \Delta\phi)$$

N^{K^-}, N^{K^+} are comparable.

$R_2^{\pi^+ K^-}(0, 0) > R_2^{\pi^+ K^+}(0, 0)$ resulting in a peak in B_{2+}



Evaluation of systematic uncertainties

Three methods to find systematic errors

Method 1

σ_{sys} of a bin is the standard deviation of the bin values of all cut sets (N) for projections of B_2 for that bin.

$$\sigma_{sys} = \sqrt{\sum_{i=1}^N \left(\frac{1}{(N-1)} (x_i - \bar{x})^2 \right)}$$

For bin 6,

$$\sigma_i = 0.00643$$



σ_{sys} of a bin is the difference in the max. and min. bin values div. by $\sqrt{12}$ of all cut sets (N) for projections of B_2 for that bin.

$$\sigma_{sys} = \frac{|x_{max} - x_{min}|}{\sqrt{12}}$$

Again, for bin 6,

$$\frac{|x_{max} - x_{min}|}{\sqrt{12}} = 6.946 \times 10^{-3}$$

$N = 4 \times 4$ cutsets: nHits \otimes gDCA

nHits	14	17	20	23
gDCA (cm)	2.2	1.8	1.4	1

Method 2

Dissimilarity d of a and b with uncertainties σ_a and σ_b is:

$$d = \frac{|a - b|}{\sqrt{(\sigma_a^2 + \sigma_b^2)/k}}$$

$k=1$ if a, b for independent samples,
 $k=2$ if a, b for similar samples (used $k=2$)

d can be interpreted by a weight w between 0 and 1 given by: $w = 1 - e^{-d^2/2}$

$$a - b \rightarrow \Delta_i = y_{var,i} - y_{default}$$

The weighted RMS (gives the final systematic error) is defined as:

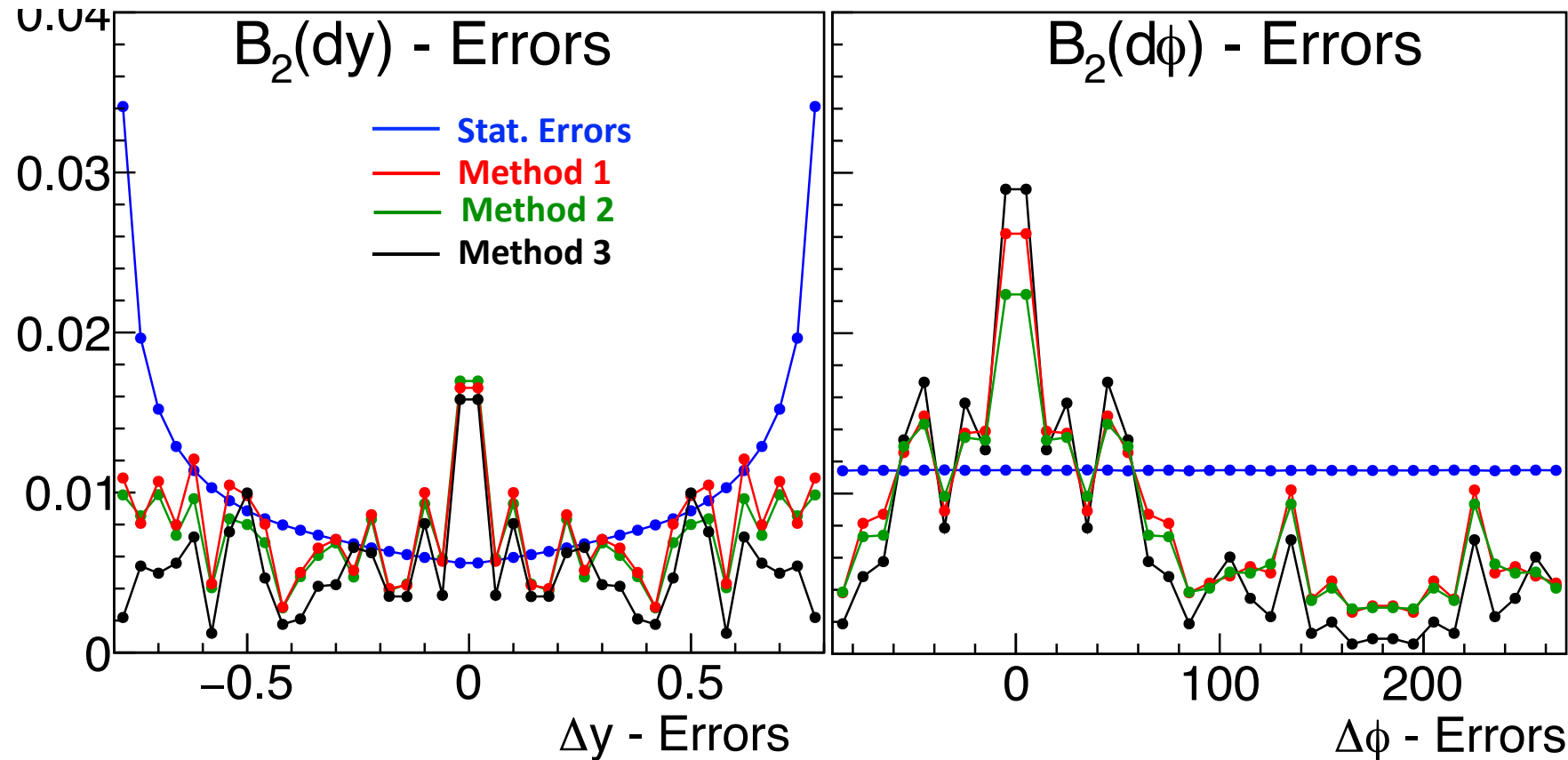
$$wRMS \stackrel{\text{def}}{=} \sqrt{\frac{1}{N_{var}} \sum_{i=1}^{N_{var}} \Delta_i^2 w_i}$$

Ref. for method 3: Thesis of Vít Kučera – “Study of strange particle production in jets with the ALICE experiment at the LHC”

Comparing the three methods for the 4x4 cutsets

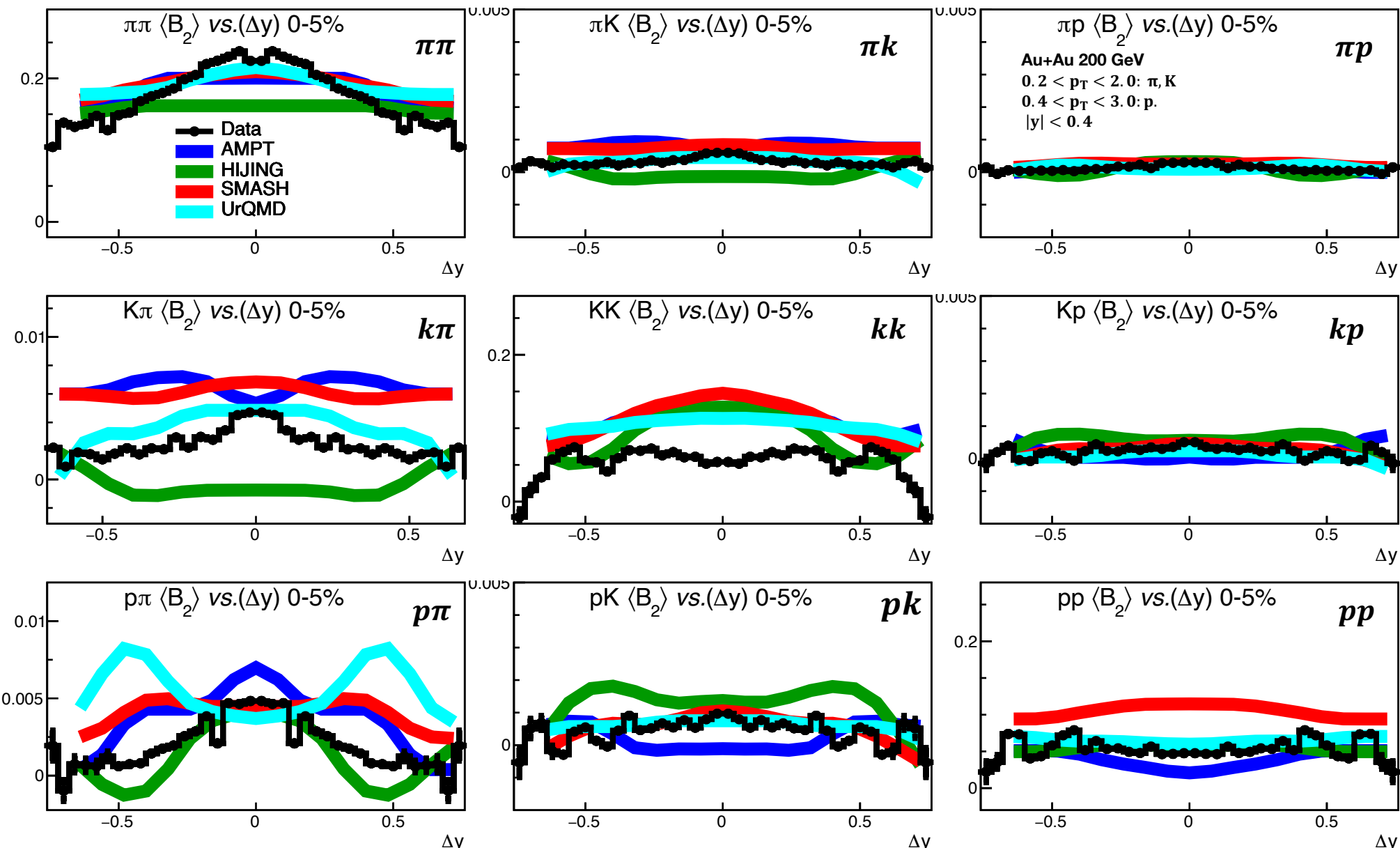
Plot of uncertainties from all 3 methods:

- Method 1 and method 2 are comparable.
- Method 3 gives larger systematic uncertainties for $B_2(d\phi)$.



Final systematic uncertainties evaluated using method 1.

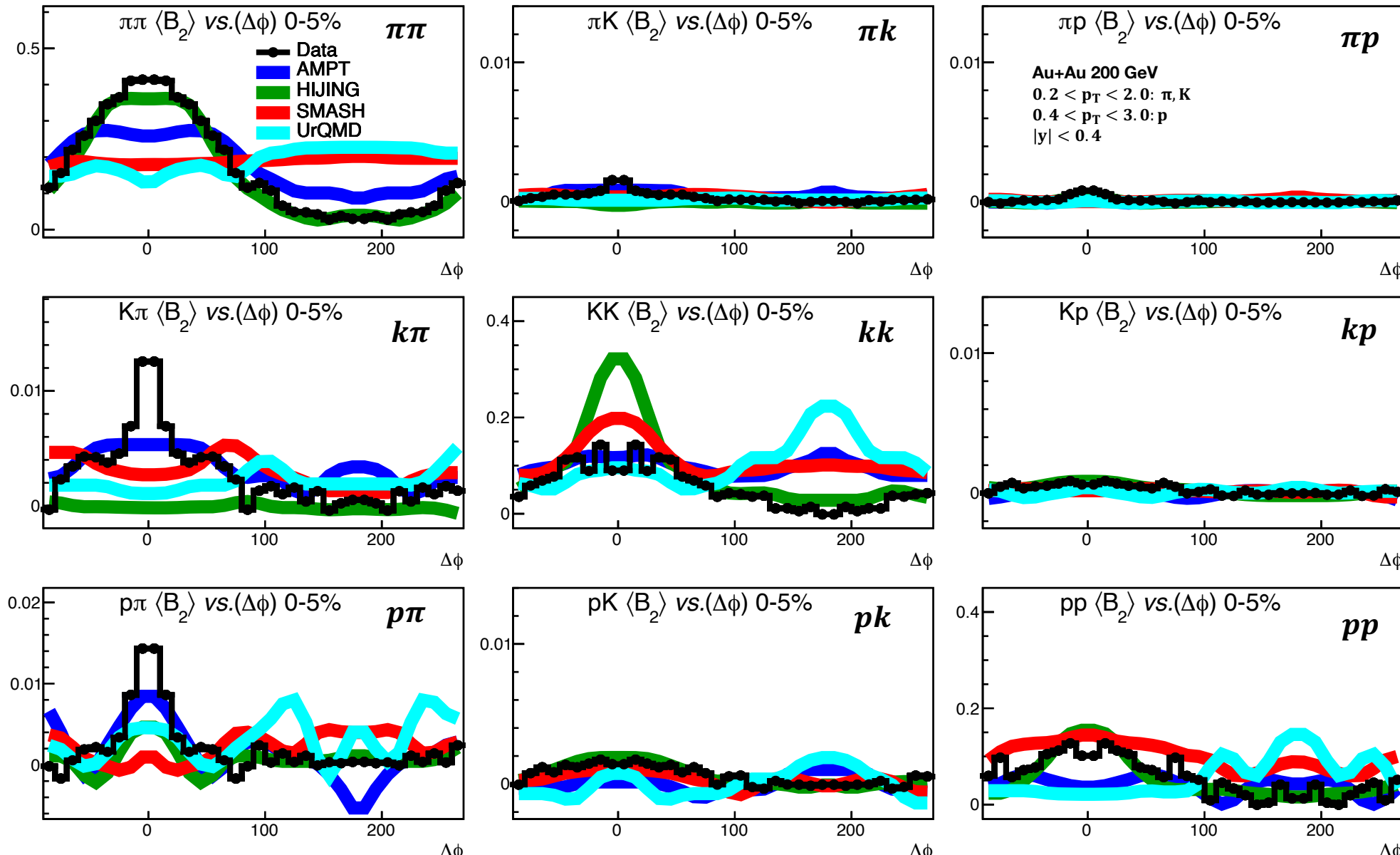
Comparison of $B_2(\Delta y)$ Model and Data for all species at 200 GeV



Comparison of $B_2(\Delta\phi)$ Model and Data for all species at 200 GeV

Uncertainties are greater for mixed species compared to the identical ones.

$B_2(\Delta\phi)$ is much smaller for mixed species compared to the identical ones (~100 times smaller in same cases).



Model details – versions, other analysis details.

- UrQMD, HIJING, and SMASH – hadronic cascade models.
- AMPT (A Multi Phase Transport) version we use is 2.26t7b – uses string melting – should be suitable for energy range from 5 GeV to 5.5 TeV. Both default (DF) and string melt (SM) use the initial conditions from HIJING (Heavy-Ion Jet INteraction Generator) + elastic parton cascade model, namely, the Zhang's Parton Cascade (ZPC)+ the Lund string model for hadronization, and the A Relativistic Transport (ART) hadron cascade. In SM version excited hadronic strings converted to partons (on top of parton cascade of the DF model)
- String: Segment b/w pairs $Q, Q_{\bar{}}\bar{}$
- Potential used in UrQMD is the sum of pot. Of nucleons/hadrons whereas in SMASH (Simulating many accelerating strongly interacting hadrons) uses a mean field potential. SMASH, UrQ, HIJ.. Good for low energy beam but AMPT for high.
- Version we use: SMASH 2.2, Hijing 1.41